

Towards modelling the central engine of short GRBs

José A. Font

Departamento de Astronomía y Astrofísica
Universidad de Valencia (Spain)



Collaborators: Luciano Rezzolla (Albert Einstein Institute, Germany)
Bruno Giacomazzo (University of Maryland, USA)
Luca Baiotti (Osaka University, Japan)
David Link (Albert Einstein Institute, Germany)



Outline of the talk

- Astrophysical motivation
- Physical and computational framework
- Earlier work on equal-mass NS simulations
- Unequal-mass NS simulations
- Summary

References: Rezzolla, Baiotti, Giacomazzo, Link & Font, CQG, **27**, 114105 (2010)
Montero, Font & Shibata, PRL, **104**, 191101 (2010)

Astrophysical motivation

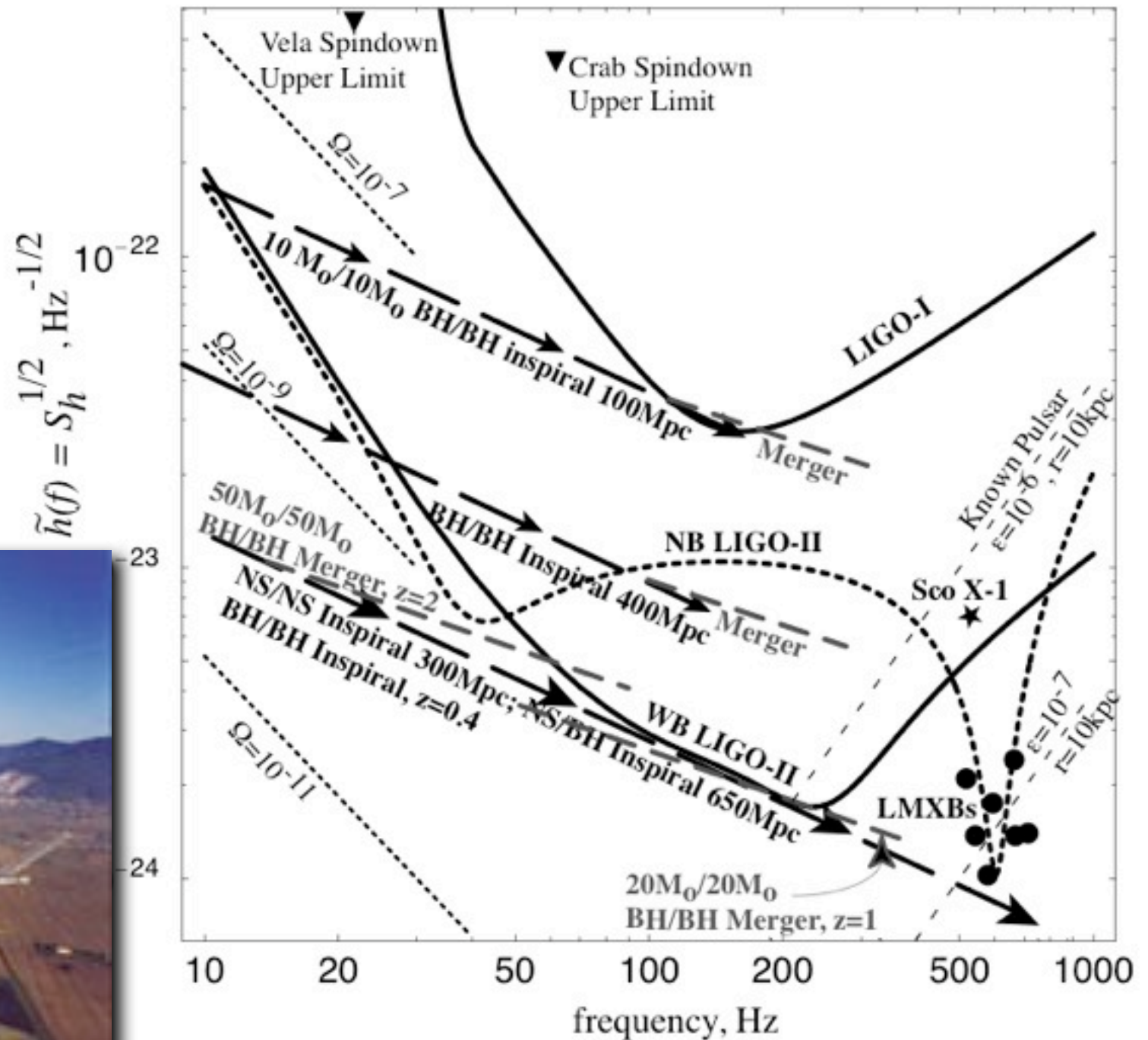
- Numerical relativity simulations of non-vacuum spacetimes have reached a status where a **complete description of the inspiral, merger and post-merger stages** of the late evolution of close binary neutron systems is **possible**.
- Determining the **properties of the black-hole-torus system** produced in such an event is a key aspect to understand the **central engine of short-hard GRBs**.
- Of the many properties characterizing the torus, the **total rest-mass** is the most important one, since it is the torus' binding energy which can be tapped to extract the large amount of energy necessary to power the GRB emission.
- In addition, the **rest-mass density and angular momentum distribution** in the torus also represent important elements which determine its secular evolution and need to be computed equally accurately for any satisfactory modelling of the GRB engine.
- This talk addresses our recent investigation of the **late-time dynamics of the torus + black hole system formed after the merger of unequal-mass neutron star binaries** (Rezzolla et al 2010). *Ab initio* modelling of the central engine of short-hard GRBs.

Why study binary neutron star mergers?

Reason #1:

Because they are among the most powerful sources of **gravitational waves** and could be the Rosetta stone in high-density nuclear physics (critical key to decipher the NS physics)

Cutler & Thorne, 03



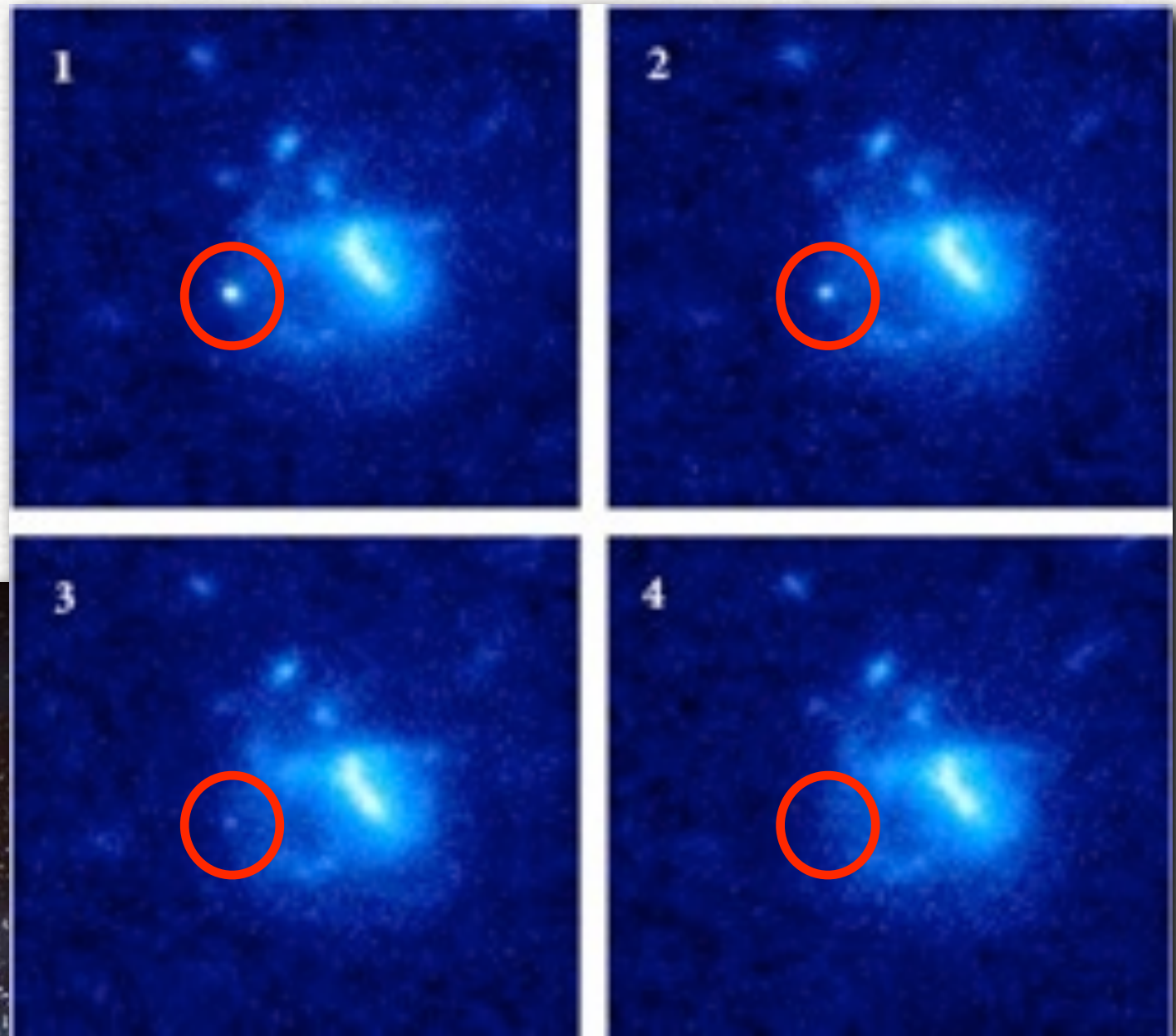
Virgo, Italy



Why study binary neutron star mergers?

Reason #2:

Because their inspiral and merger could be behind one of the most powerful phenomena in the universe: **short Gamma Ray Bursts (GRBs)**

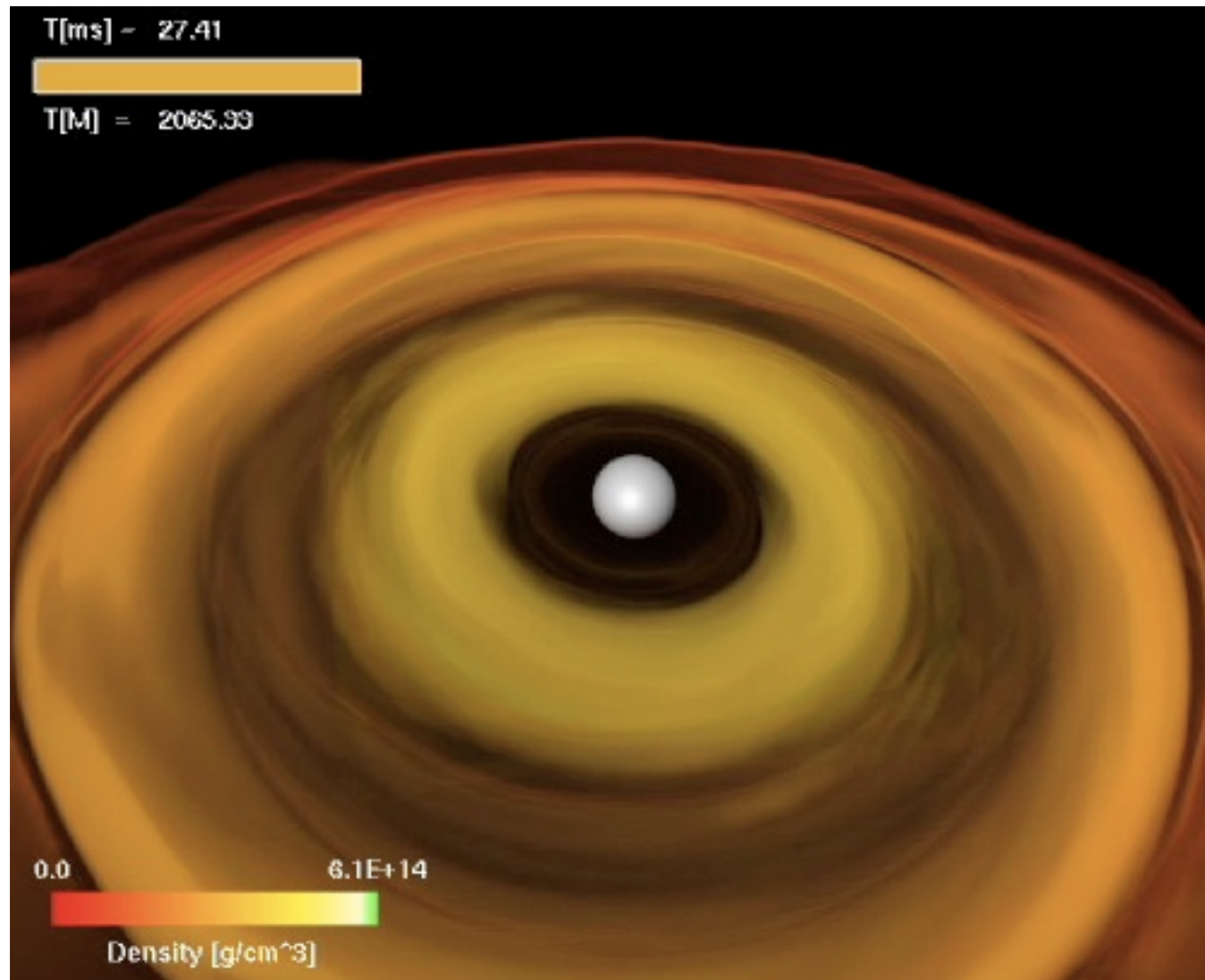


HST images of July 9, 2005 GRB taken 5.6, 9.8, 18.6 & 34.7 days after the burst (Derek Fox, Penn State University)

short GRB, artist impression, NASA



Black hole + torus system



Numerical simulations of NS-NS (i.e. Shibata et al, Baiotti et al. 2008) show that most of the material disappears beyond the event horizon in a few ms.

As a result, a **thick accreting disk or torus with mass of about 10% of total mass (upper limit) may be formed.**

These type of astrophysical objects are very interesting because **most current models for the central engine of GRBs** involve an accretion torus orbiting around a central black hole.

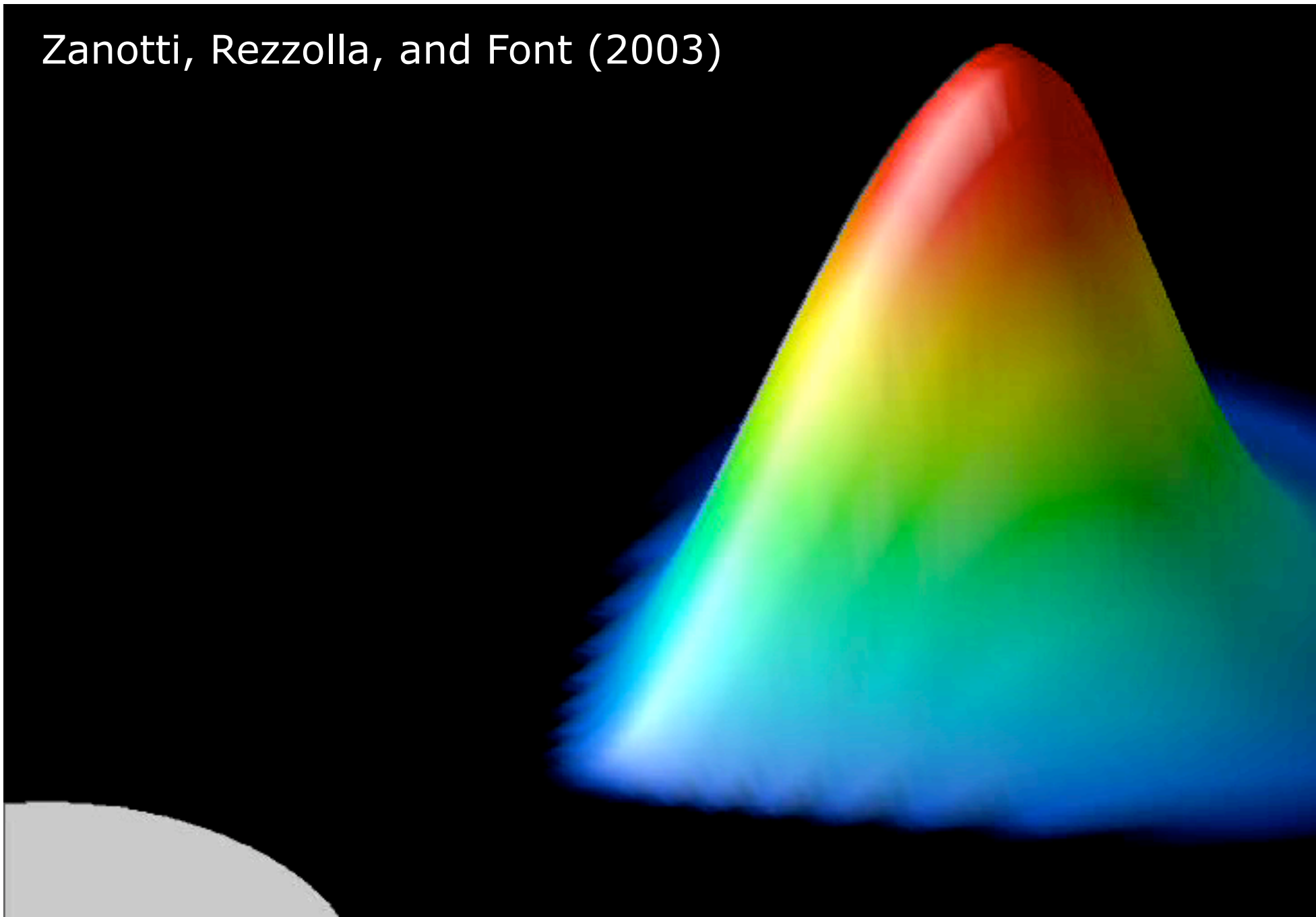
Thus, it is important to investigate its **stability properties.**

And also because these objects may also be a **promising source of gravitational radiation.**

Oscillating tori as gravitational wave source

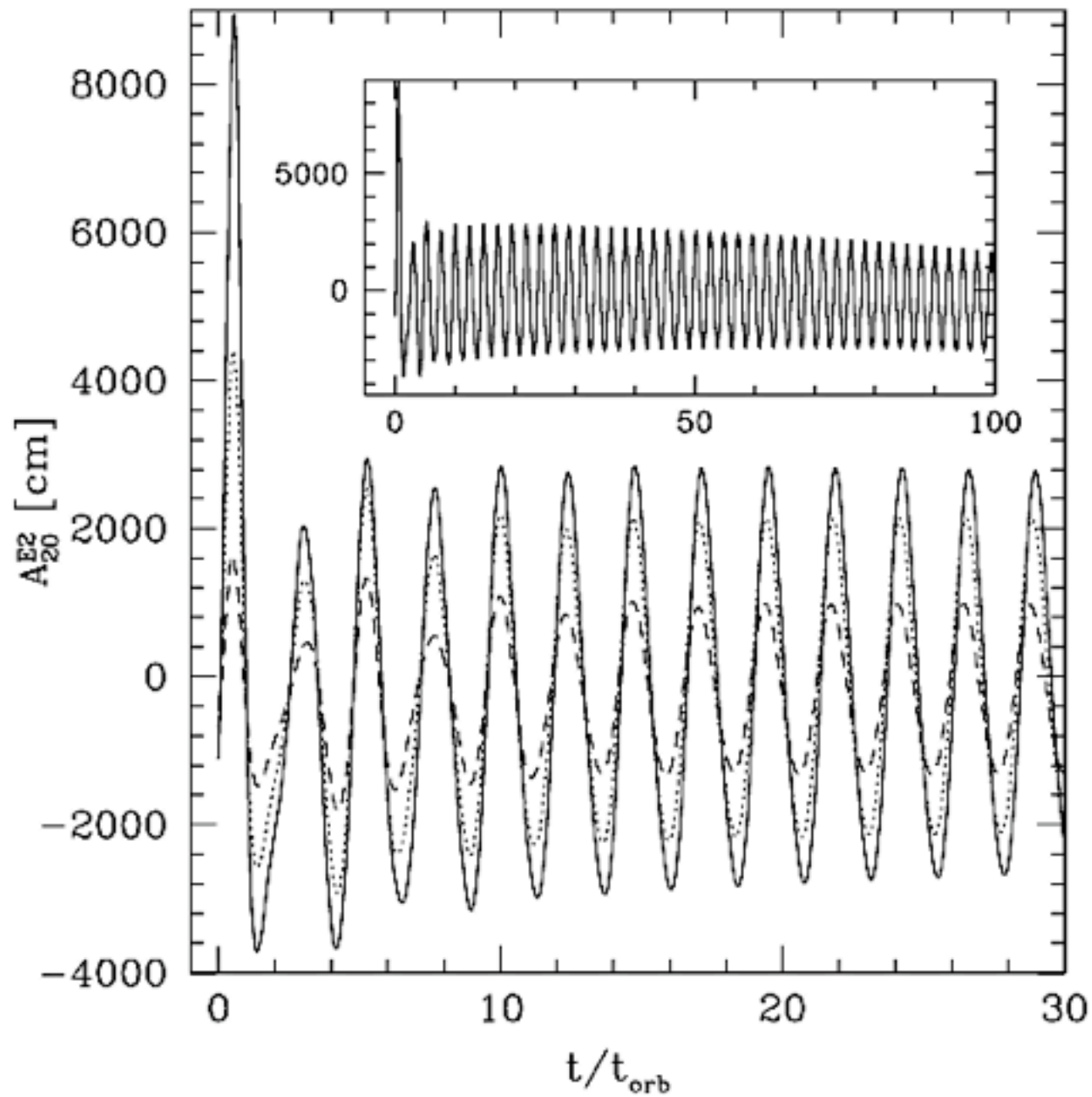
General relativistic hydrodynamical (and MHD) “test-fluid” simulations have shown that **high density relativistic tori** (around Schwarzschild or Kerr black holes) and **subject to perturbations, undergo a persistent oscillation phase and are a promising new source of GWs.**

Zanotti, Rezzolla, and Font (2003)

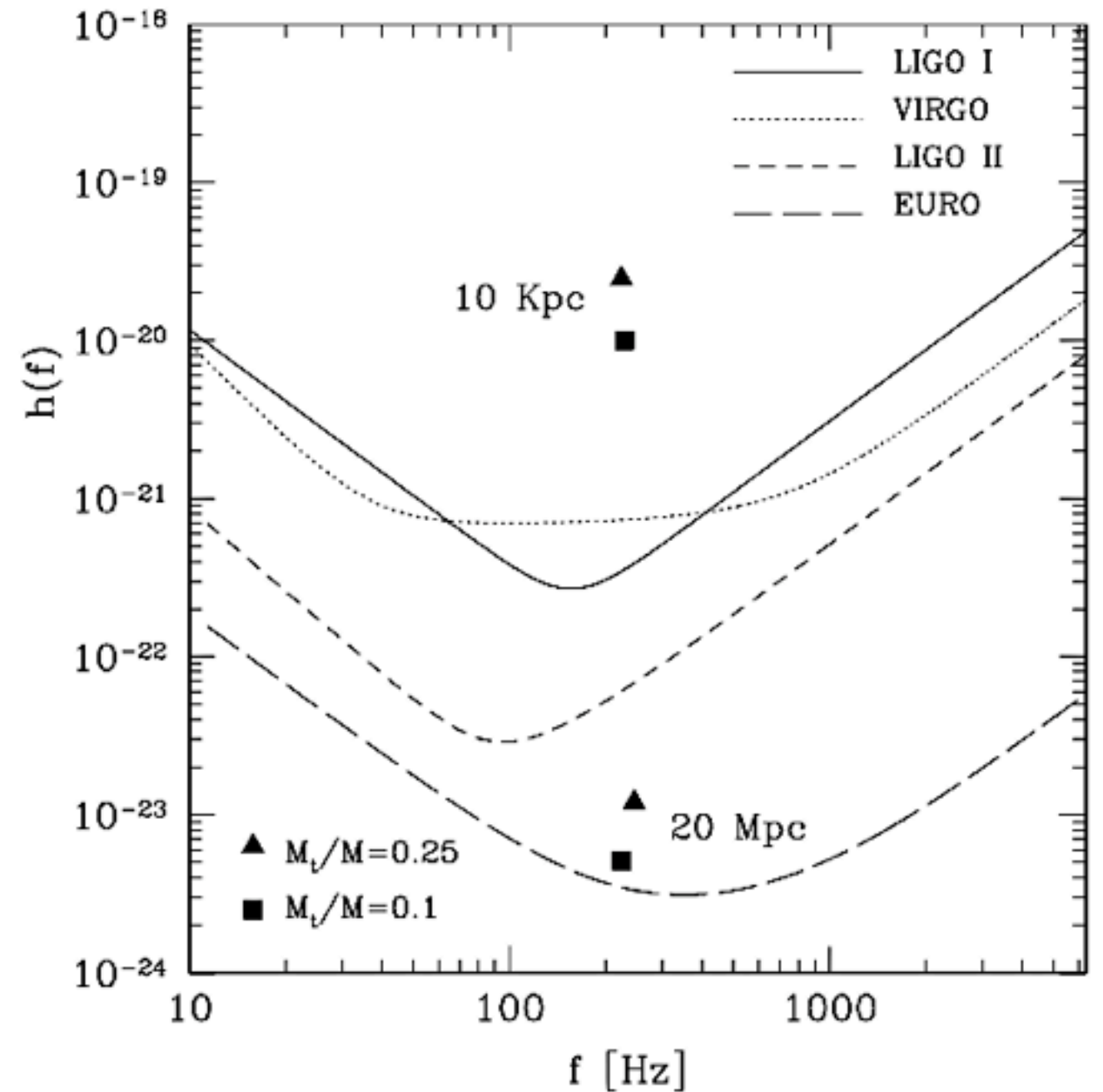


Accretion tori as gravitational wave source

Time evolution of mass quadrupole



Gravitational wave amplitude



Zanotti, Rezzolla, and Font (2003)

GRB mechanism in a nutshell



In a GRB the **energy supply** comes from the energy released by the **accretion of disk material** onto the BH and from the **rotational energy of the BH** itself, which can be extracted, for instance, via the Blandford-Znajek mechanism.

This vast amount of energy (of the order of 10^{53} – 10^{54} erg, depending on the mass of the disk and on the BH rotation and mass) is sufficient to power a GRB if **the energy released can be converted into gamma-rays with an efficiency of about a few percent.**

This scenario requires a **stable enough system to survive for a few seconds.** In particular, the internal-shock model (Rees & Meszaros 1994) implies that the duration of the energy release by the source has a duration comparable with the observed duration of the GRB.

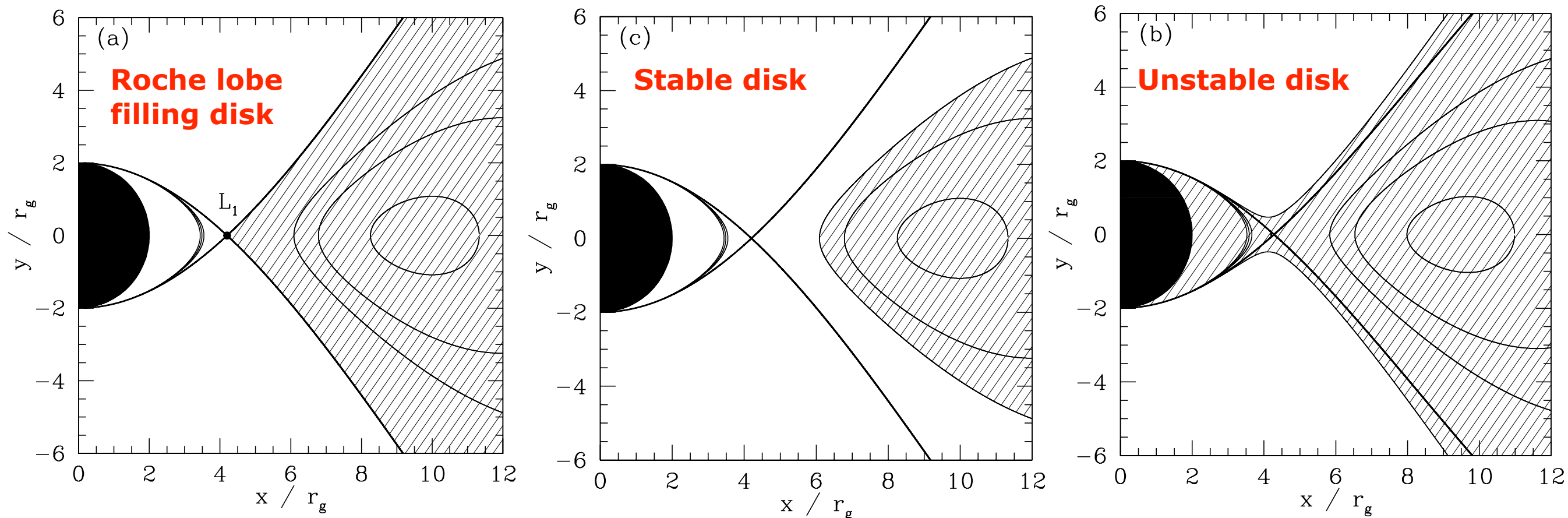
Any instability which might disrupt the system on shorter timescales, such as the so-called **runaway instability**, could pose a severe problem for the accepted GRB models.

The runaway instability

In a black hole + thick disk system the gas flows in an effective (gravitational + centrifugal) potential whose structure is similar to that of a close binary. The Roche torus has a cusp-like inner edge at the Lagrange point L_1 where mass transfer driven by the radial pressure gradient is possible.

These systems may be subjected to a **runaway instability** (Abramowicz et al 1983): due to accretion from the disk the BH mass and spin increase and the gravitational field changes. Two evolutions feasible to reach new equilibrium solution:

1. Cusp moves inwards toward the BH, mass transfer slows down. **Stable.**
2. Cusp moves deeper inside the disc material, mass transfer speeds up. **Unstable.**



Double neutron star binaries exist in Nature

| Name | M_1/M_{sun} | M_2/M_{sun} | $q=M_2/M_1$ |
|------------|----------------------|----------------------|-------------|
| B1534+12 | 1.33 | 1.34 | 0.99 |
| B2127+11C | 1.36 | 1.35 | 0.99 |
| B1913+16 | 1.44 | 1.38 | 0.96 |
| J0737-3039 | 1.33 | 1.25 | 0.94 |
| J1906+0746 | 1.35 | 1.26 | 0.93 |
| J1829+2456 | 1.14 | 1.36 | 0.84 |
| J1756-2251 | 1.40 | 1.18 | 0.84 |
| J1811-1736 | 1.62 | 1.11 | 0.69 |
| J1518+4904 | 1.56 | 1.05 | 0.67 |

Stairs 2004

Equations to solve: Einstein, hydro/MHD, EOS, ...

This is not yet astrophysics but our approximation to "reality".

$$R_{\mu\nu} - \frac{1}{2}g_{\mu\nu}R = 8\pi T_{\mu\nu} \quad (\text{field eqs : } 6 + 6 + 3 + 1)$$

$$\nabla_{\mu}T^{\mu\nu} = 0, \quad (\text{cons. en./mom. : } 3 + 1)$$

$$\nabla_{\mu}(\rho u^{\mu}) = 0, \quad (\text{cons. of baryon no : } 1)$$

$$p = p(\rho, \epsilon, \dots). \quad (\text{EoS : } 1 + \dots)$$

Still very crude but it can be improved: microphysics for the EOS, magnetic fields, viscosity, radiation transport,...

$$\nabla_{\nu}^*F^{\mu\nu} = 0, \quad (\text{Maxwell eqs. : induction, zero div.})$$

$$T_{\mu\nu} = T_{\mu\nu}^{\text{fluid}} + T_{\mu\nu}^{\text{em}} + \dots$$

Numerical framework for the simulations

Evolution field eqs (www.cactuscode.org)

Use a **conformal** and **traceless** "3+1" formulation of Einstein equations

Gauge conditions: "1+log" slicing for **lapse**; hyperbolic "Gamma-driver" for shift

Use consistent configurations of "**irrotational**" binary NSs in quasi-circular orbit

Use **4th-8th** order finite-differencing

Wave-extraction with **Weyl scalars** and **gauge-invariant perturbations**

HD/MHD eqs (www.whiskycode.org)

HRSC methods with a variety of approx Riemann solvers (HLLE, Roe, Marquina, etc.) and reconstructions (PPM, minmod, TVD, etc.)

Method of lines for time integration

Use **excision** if needed

Use of suitable techniques for constraining the magnetic field to be divergence-free

AMR with moving grids (www.carpetcode.org)

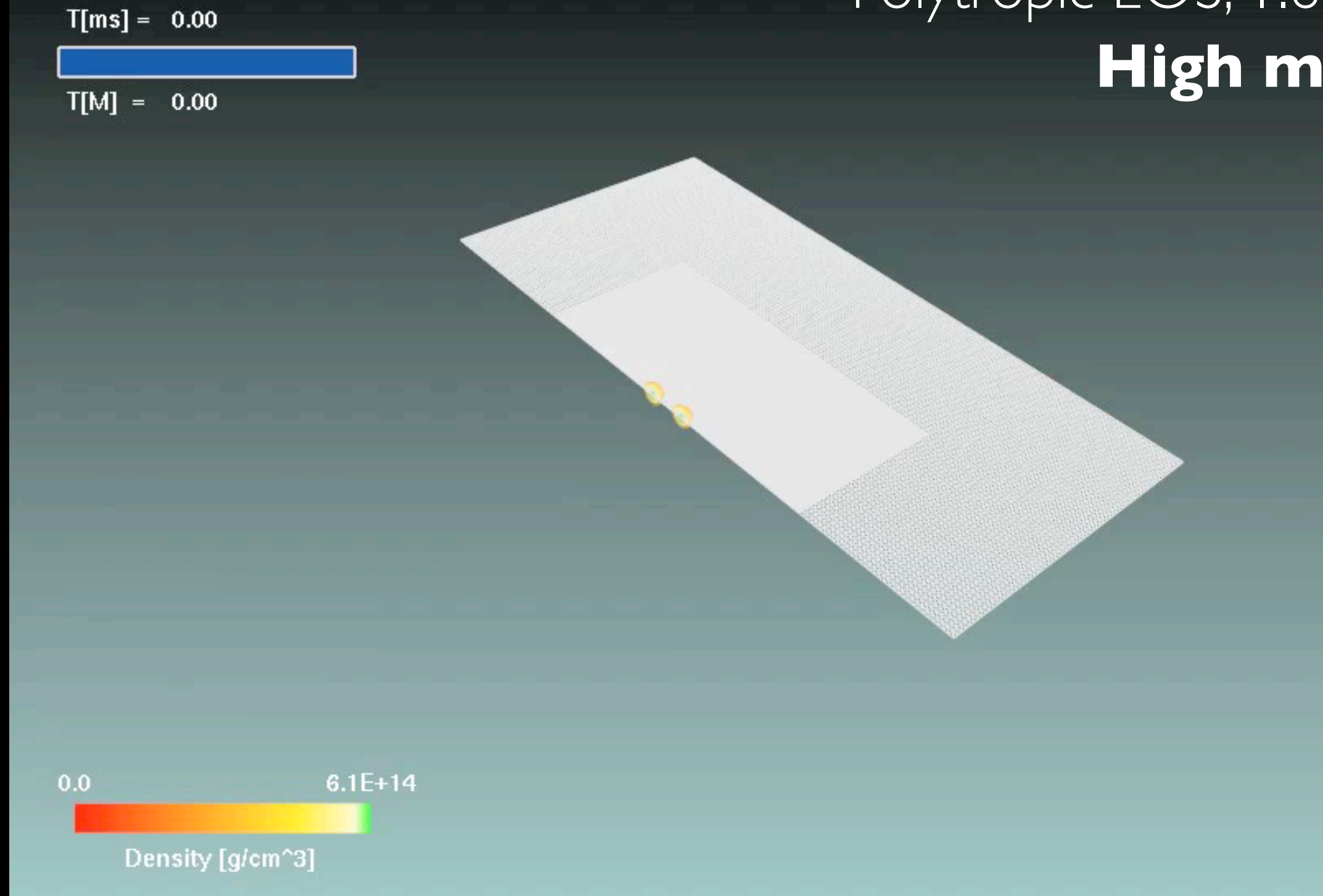
Previous work on NS/NS mergers

The numerical investigation of the coalescence and merger of binary neutron stars within the framework of general relativity is receiving **increasing attention in recent years** (e.g. Shibata & Taniguchi 2006, Anderson et al 2008, Baiotti et al 2008, 2009, Liu et al 2008, Giacomazzo et al 2009, Kiuchi et al 2009, Rezzolla et al 2010).

Drastic **improvements** in the simulation front regarding **mathematics** (e.g. formulation of the equations), **physics** (e.g. incorporation of equations of state from nuclear physics and MHD), and **numerical methods** (e.g. use of high-resolution methods and adaptive mesh refinement), along with increased **computational resources**, have allowed to extend the scope of the early simulations (e.g. Shibata and Uryu 2000).

Larger initial separations have recently started being considered and some of the existing simulations have expanded the range spanned by the models well **beyond black-hole formation** (Baiotti et al 2008, Kiuchi et al 2009, Giacomazzo et al 2009, Rezzolla et al 2010).

Polytropic EOS, 1.6 M_{\odot}
High mass



A hot, low-density torus is produced orbiting around the BH.
This is what is expected in short GRBs. (Baiotti et al 2008)

The behaviour:

“merger \longrightarrow HMNS \longrightarrow BH + torus”

is general but only qualitatively

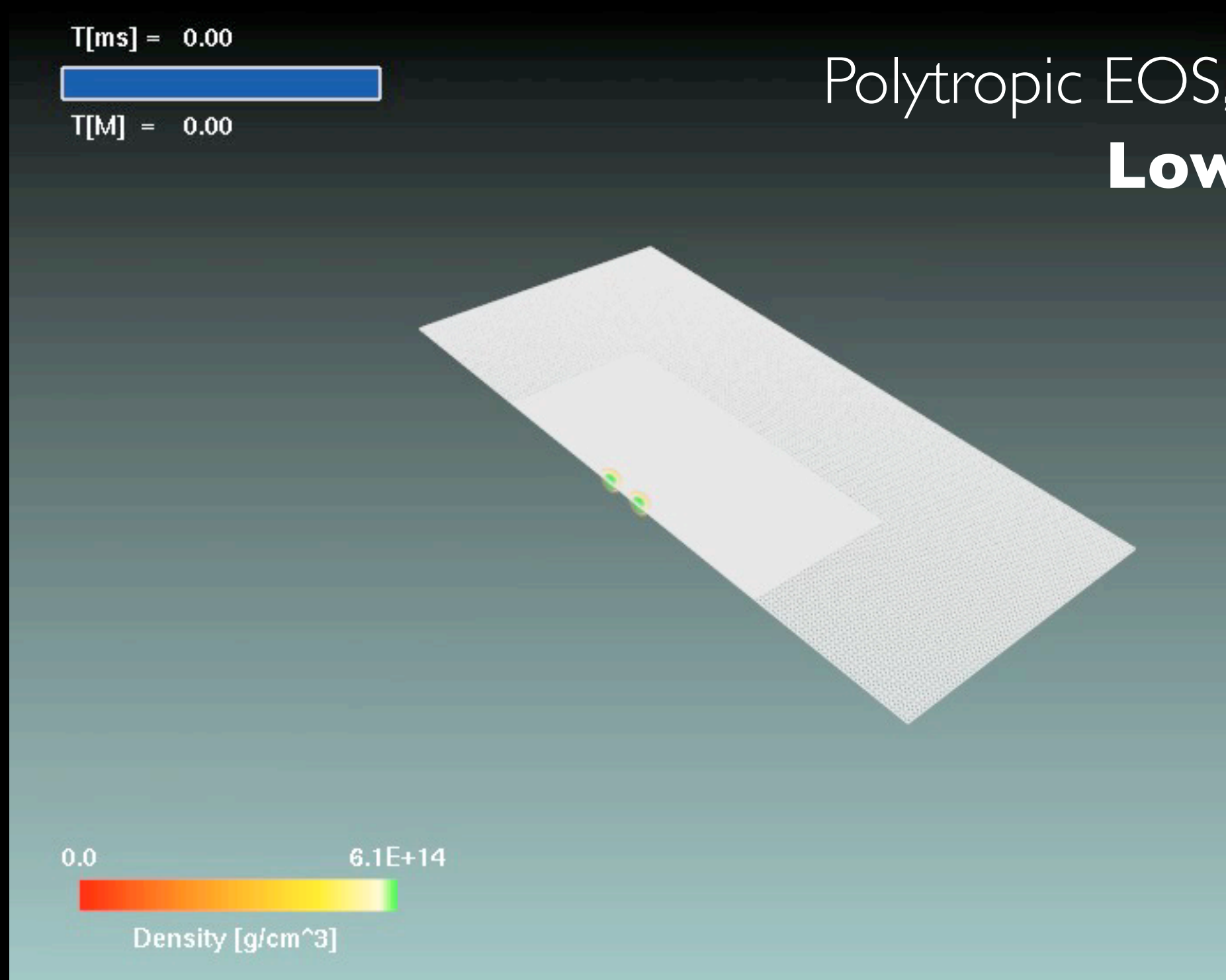
Quantitative differences are produced by:

- differences in the mass for the same EOS:

a binary with smaller mass will produce a HMNS which is further away from the stability threshold and will collapse at a later time

- differences in the EOS for the same mass:

a binary with an EOS allowing for a larger thermal internal energy (ie hotter after merger) will have an increased pressure support and will collapse at a later time

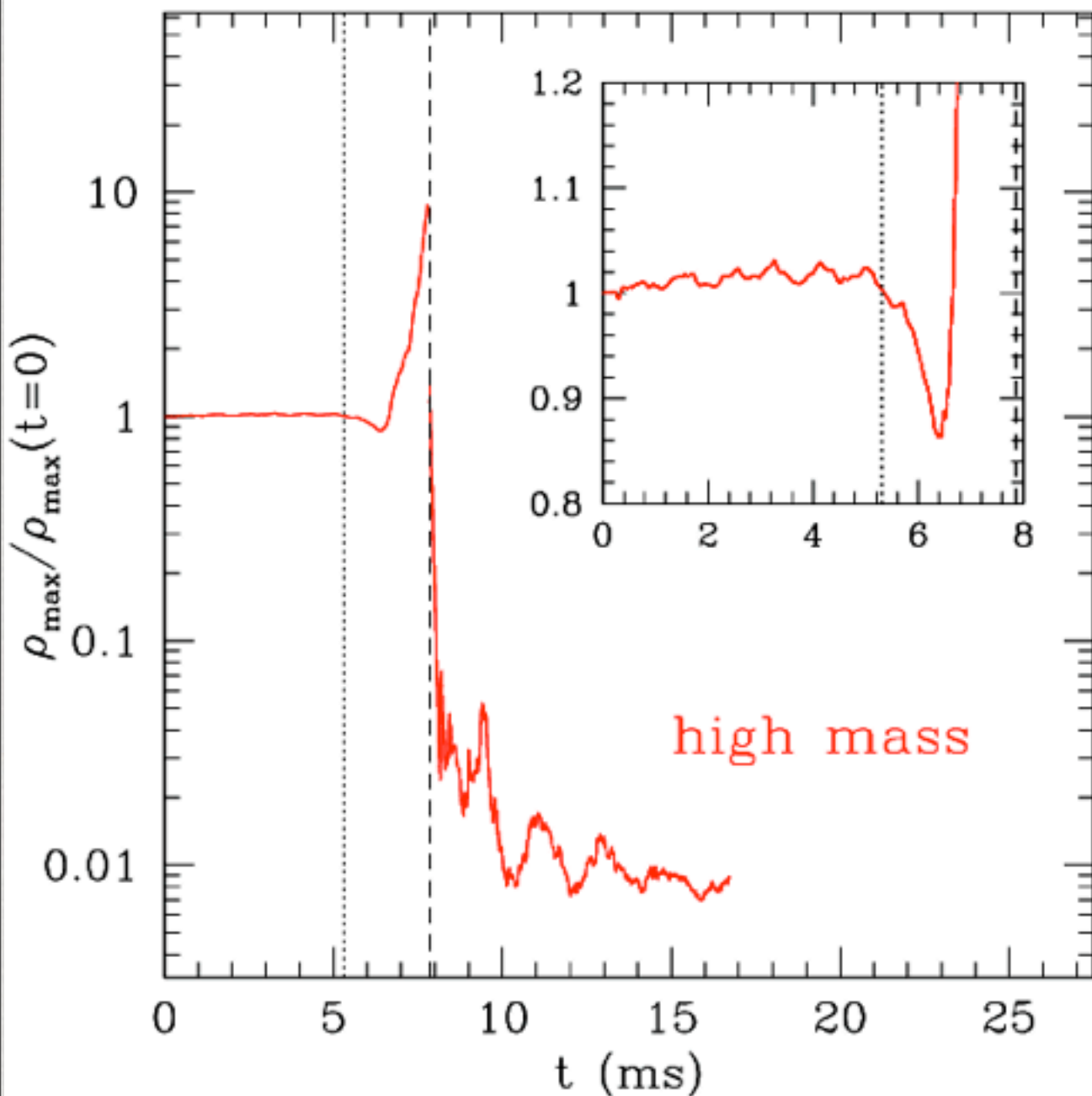


The HMNS is far from the instability threshold and survives for a longer time while losing energy and angular momentum.

After ~ 25 ms the HMNS has lost sufficient angular momentum and will collapse to a BH.

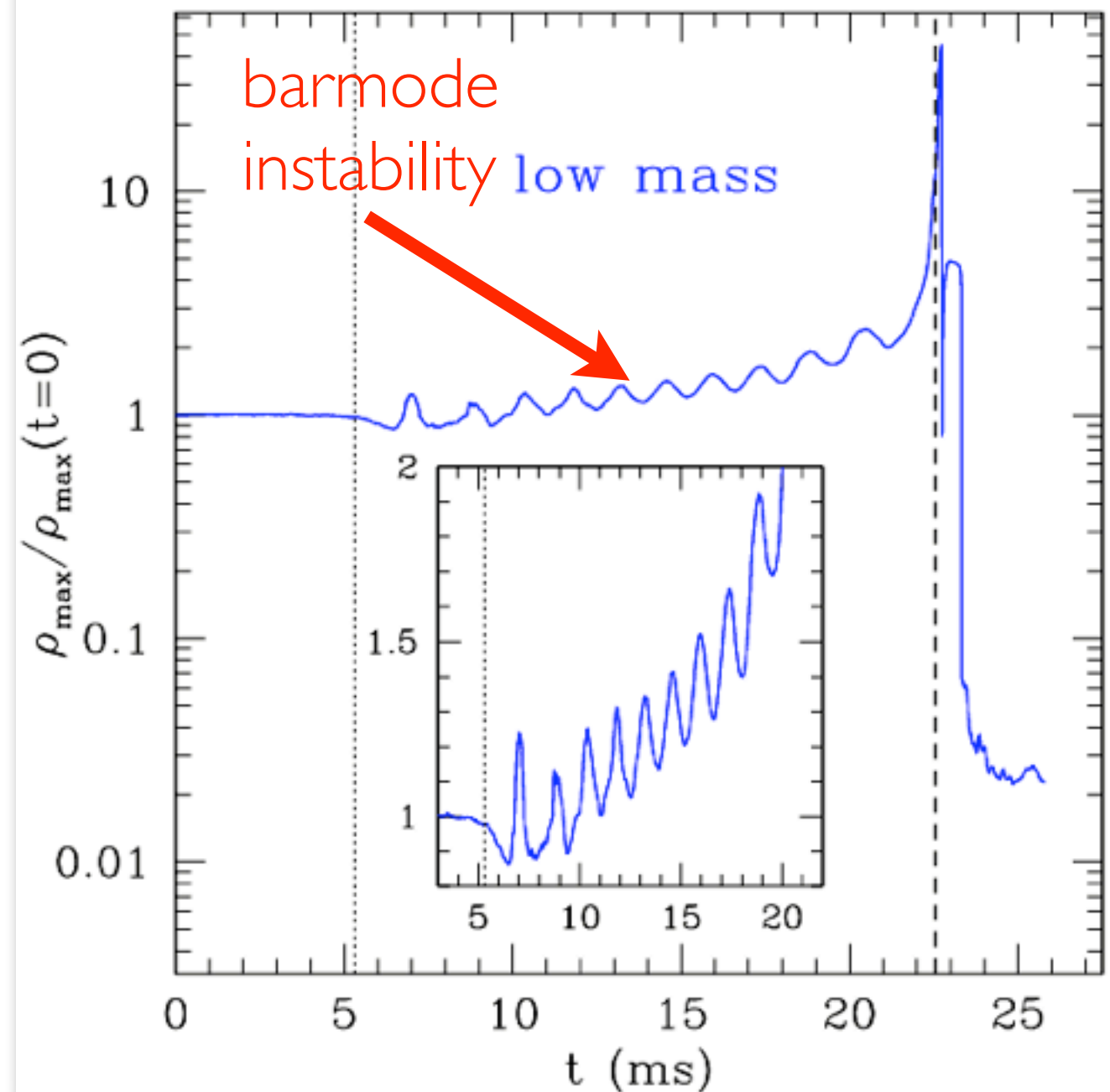
Matter dynamics comparison

high-mass binary



soon after the merge the torus is formed and undergoes oscillations

low-mass binary

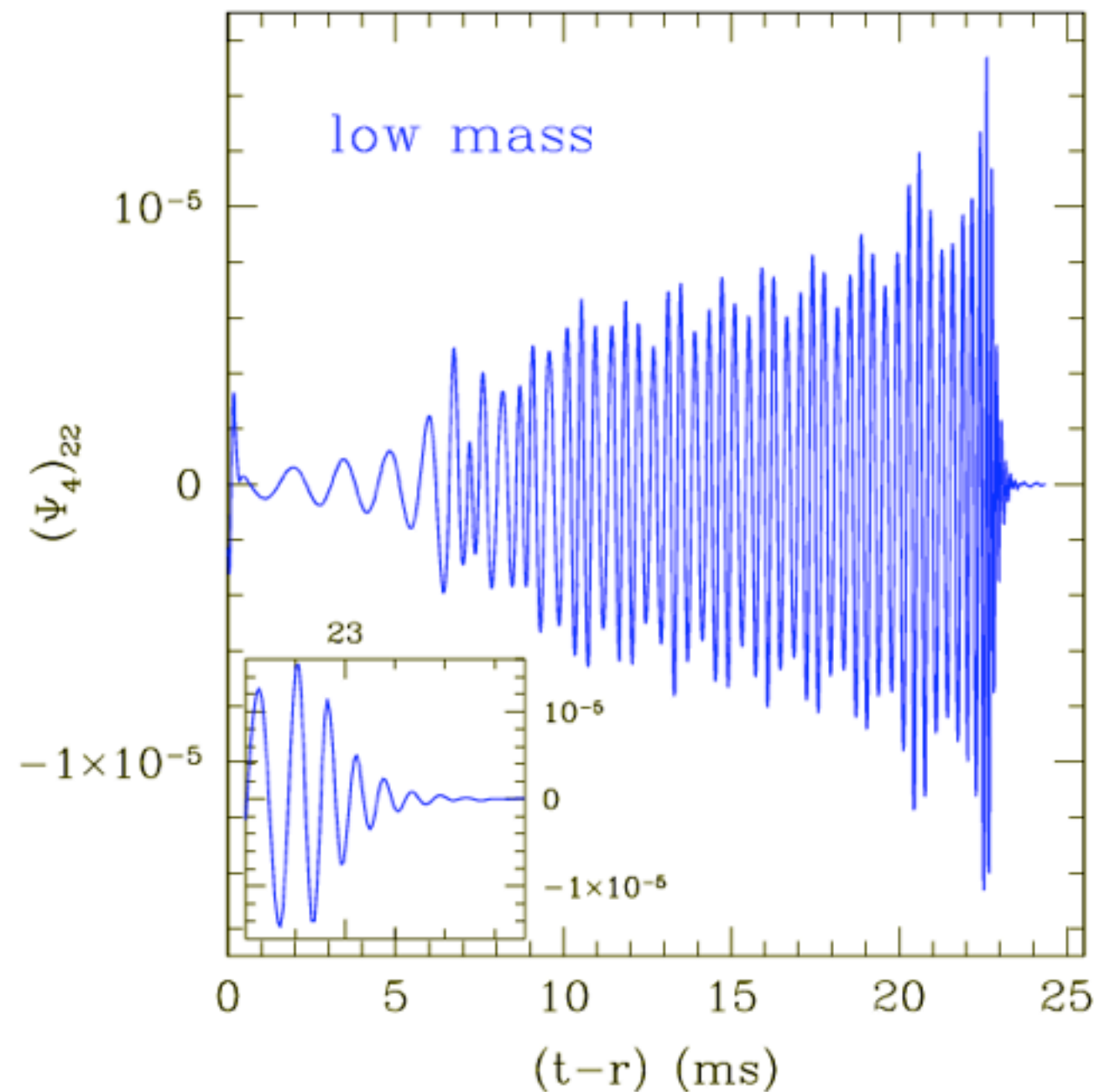
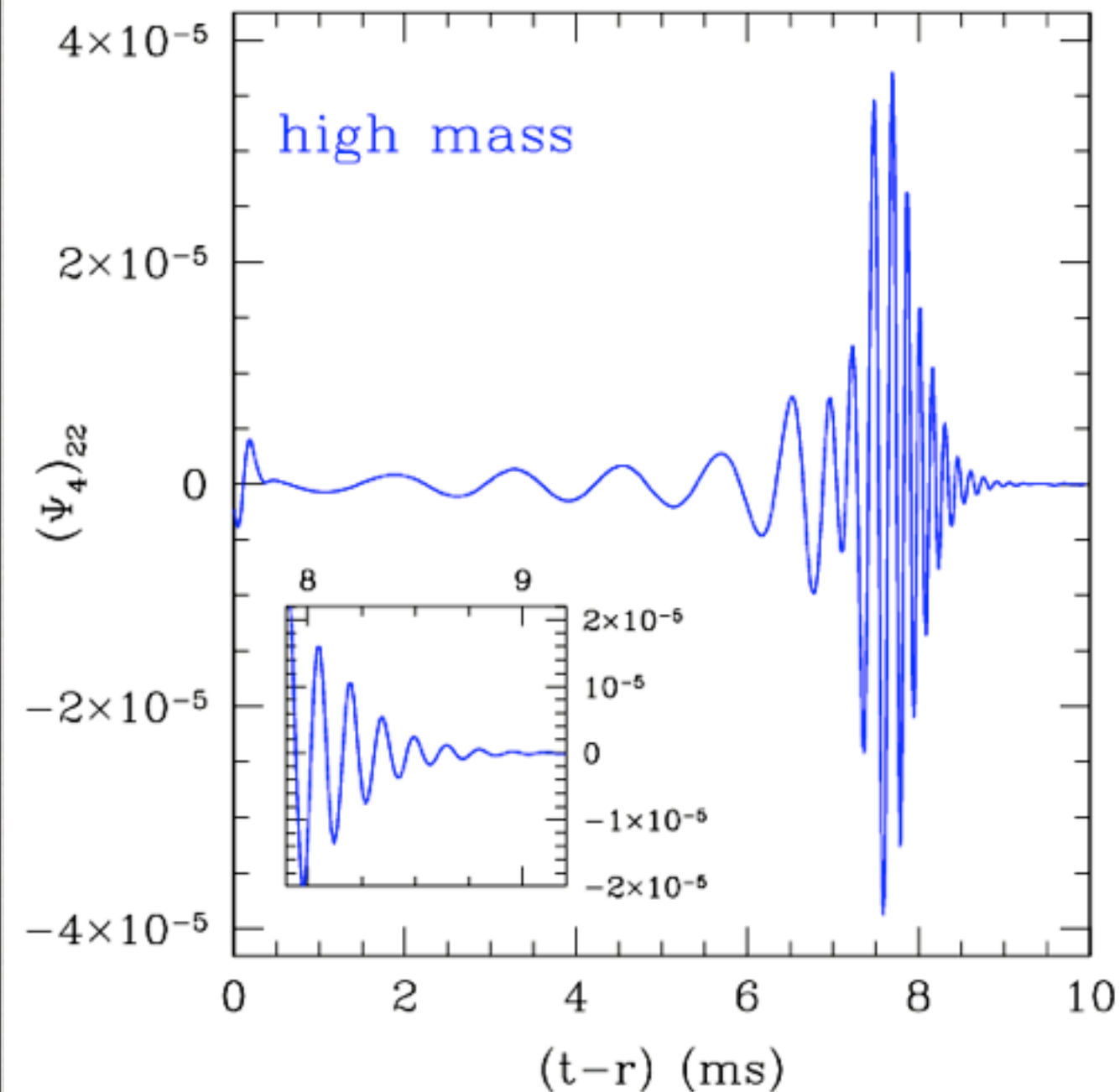


long after the merger a BH is formed surrounded by a torus

Gravitational waveforms comparison: polytropic EOS

high-mass binary

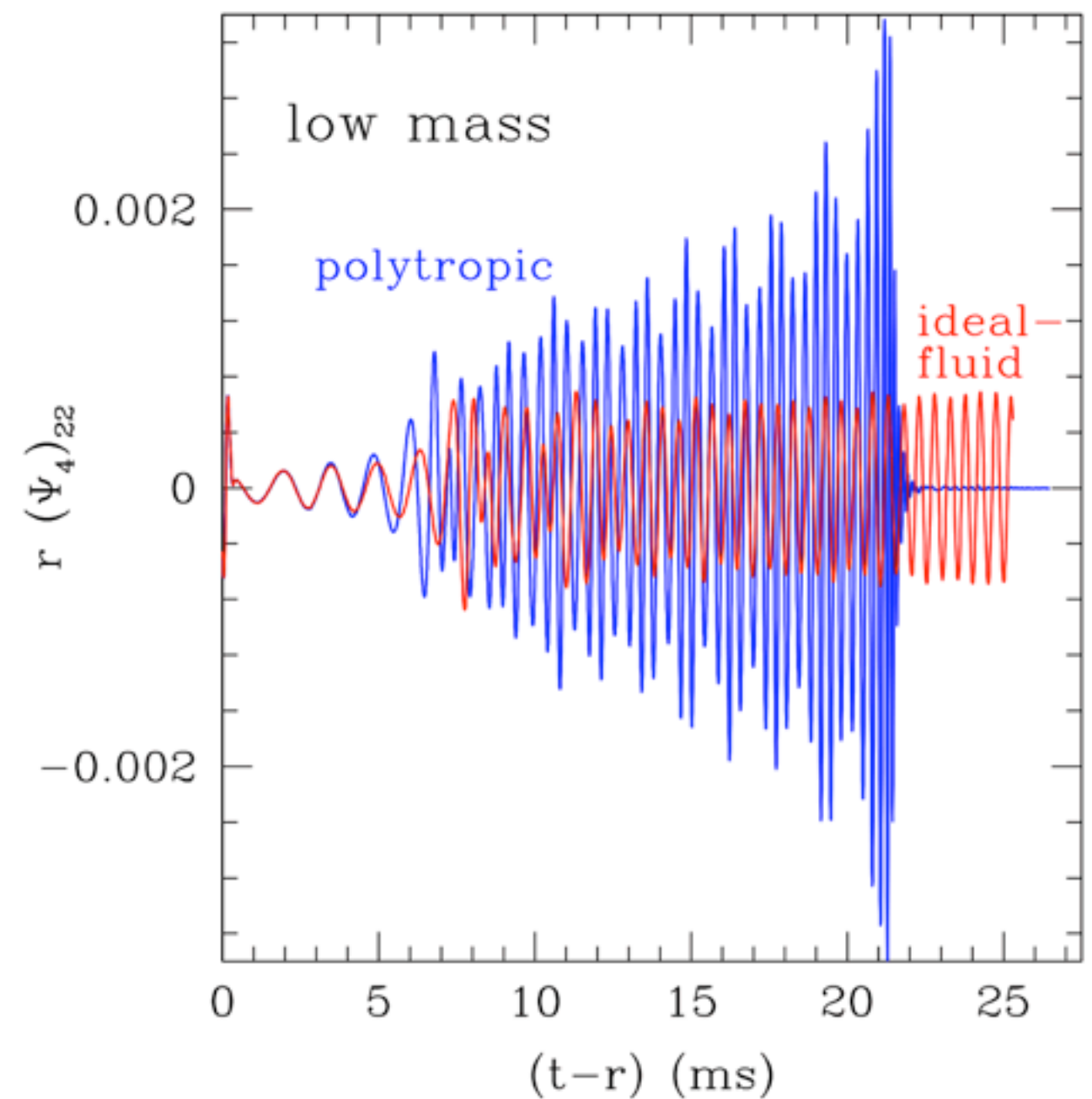
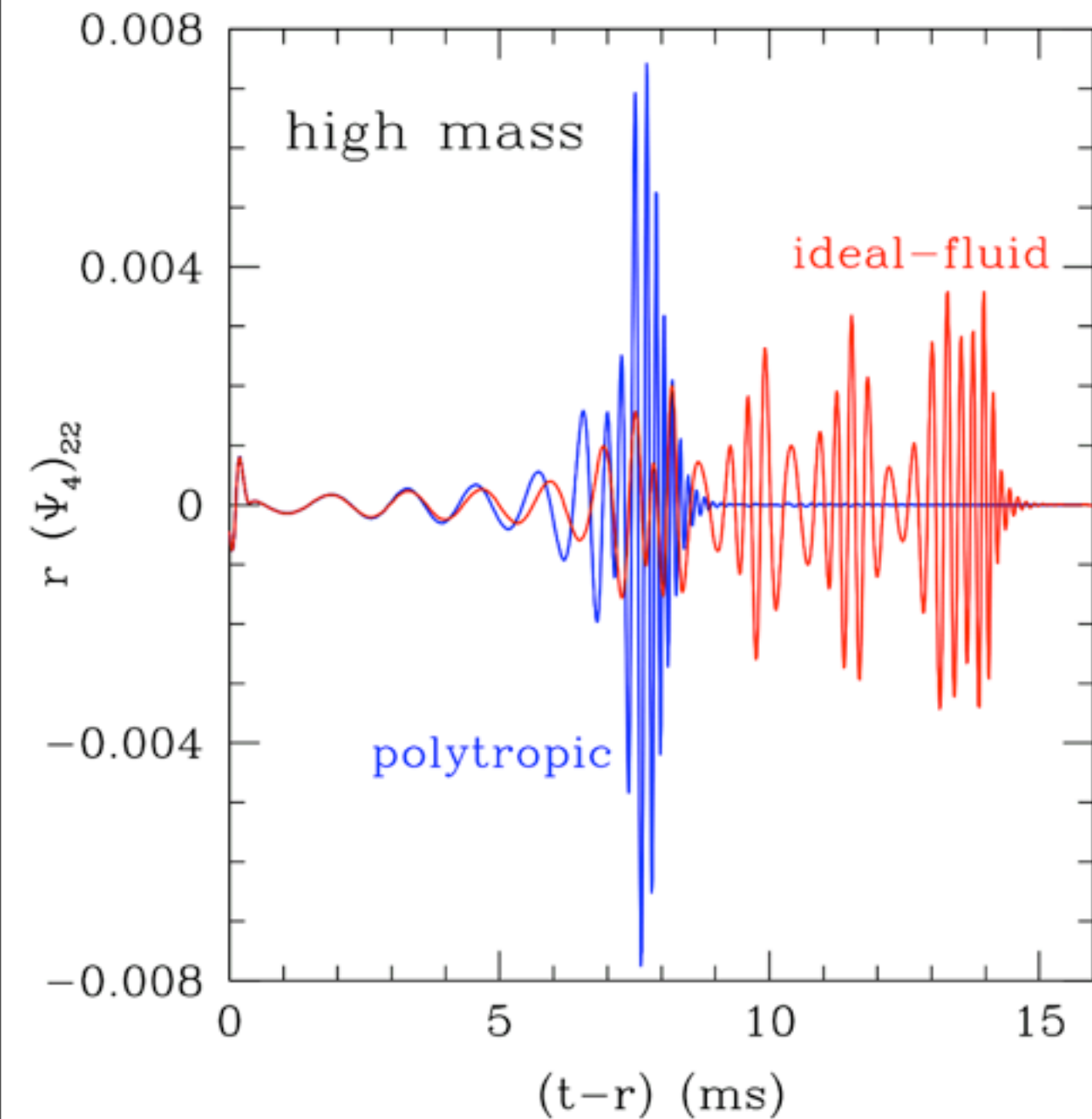
low-mass binary



first time the full signal from the formation to a bh has been computed

development of a bar-deformed NS leads to a long gw signal

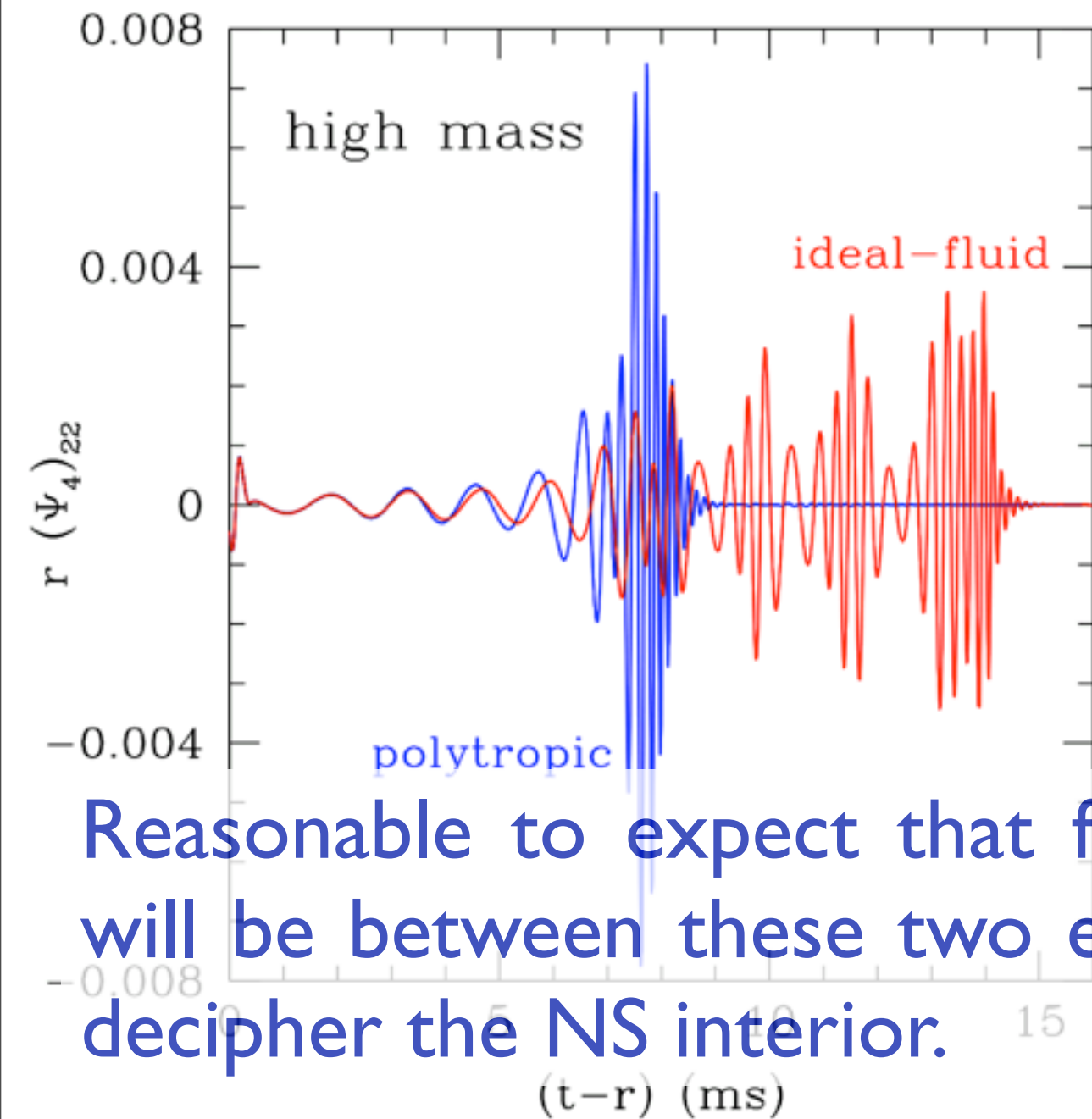
Imprint of the EOS: Ideal fluid vs polytropic



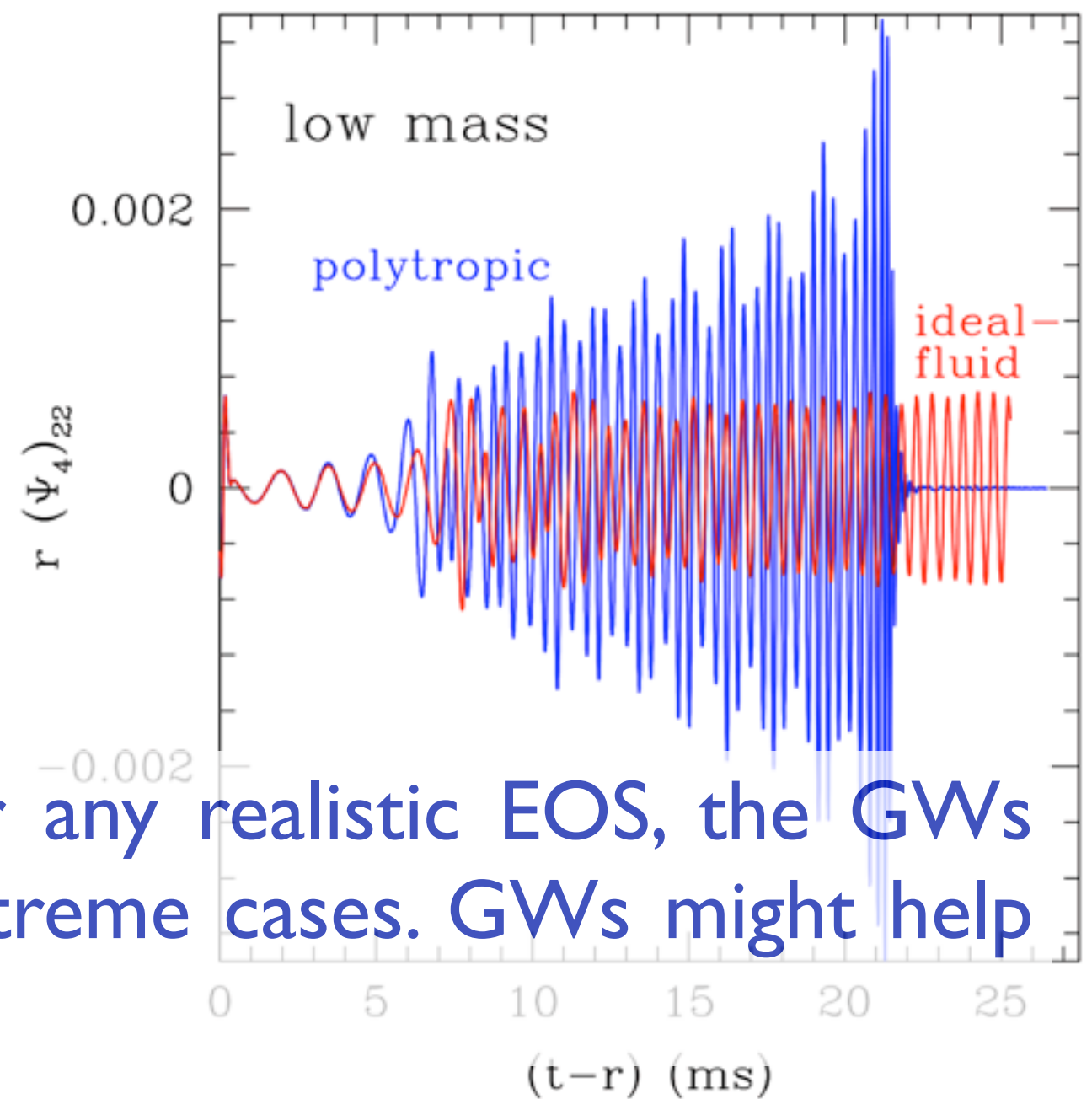
After the merger a BH is produced over a timescale **comparable** with the **dynamical** one

After the merger a BH is produced over a timescale **larger** or **much larger** than the **dynamical** one

Imprint of the EOS: Ideal fluid vs polytropic



Reasonable to expect that for any realistic EOS, the GWs will be between these two extreme cases. GWs might help decipher the NS interior.



After the merger a BH is produced over a timescale larger or much larger than the dynamical one

After the merger a BH is produced over a timescale comparable with the dynamical one

Initial data for unequal-mass neutron stars

| Model | $M_{\text{tot}}, M_{\text{ADM}}$ (M_{\odot}) | q, q_{ADM} | $J/10^{49}$ ($\text{g cm}^2/\text{s}$) | ν_{orb} (Hz) | $\rho_{\text{max}}/10^{14}$ (g/cm^3) | \bar{r}_2, \bar{r}_1 (km) | \bar{A}_2, \bar{A}_1 | $M_1^{\infty}, M_2^{\infty}$ (M_{\odot}) | $C_1^{\infty}, C_2^{\infty}$ |
|-----------|---|---------------------|---|----------------------------|--|--------------------------------|------------------------|---|------------------------------|
| M3.6q1.00 | 3.56, 3.23 | 1.00, 1.00 | 8.92 | 303.32 | 7.58 | 12.0, 12.0 | 0.95, 0.95 | 1.643, 1.643 | 0.130, 0.130 |
| M3.7q0.94 | 3.68, 3.33 | 0.94, 0.94 | 9.37 | 306.56 | 9.75 | 12.0, 11.0 | 0.95, 0.96 | 1.643, 1.742 | 0.130, 0.150 |
| M3.4q0.91 | 3.40, 3.11 | 0.91, 0.92 | 8.33 | 299.06 | 7.58 | 13.1, 12.1 | 0.93, 0.95 | 1.512, 1.643 | 0.111, 0.130 |
| M3.4q0.80 | 3.37, 3.08 | 0.80, 0.81 | 8.36 | 303.62 | 9.21 | 13.8, 11.3 | 0.90, 0.97 | 1.400, 1.723 | 0.097, 0.146 |
| M3.5q0.75 | 3.46, 3.14 | 0.75, 0.77 | 8.40 | 300.84 | 12.7 | 13.0, 10.1 | 0.89, 0.98 | 1.390, 1.804 | 0.096, 0.171 |
| M3.4q0.70 | 3.37, 3.07 | 0.70, 0.72 | 7.98 | 298.47 | 12.8 | 14.6, 10.0 | 0.85, 0.98 | 1.304, 1.805 | 0.087, 0.172 |



Mass ratio.

Total baryonic mass: high enough to lead to prompt collapse to BH.

All the initial models are computed using the **Lorene code** for unmagnetized binary neutron stars (Bonazzola et al. 1999; www.lorene.obspm.fr).

Technical data for the simulations:

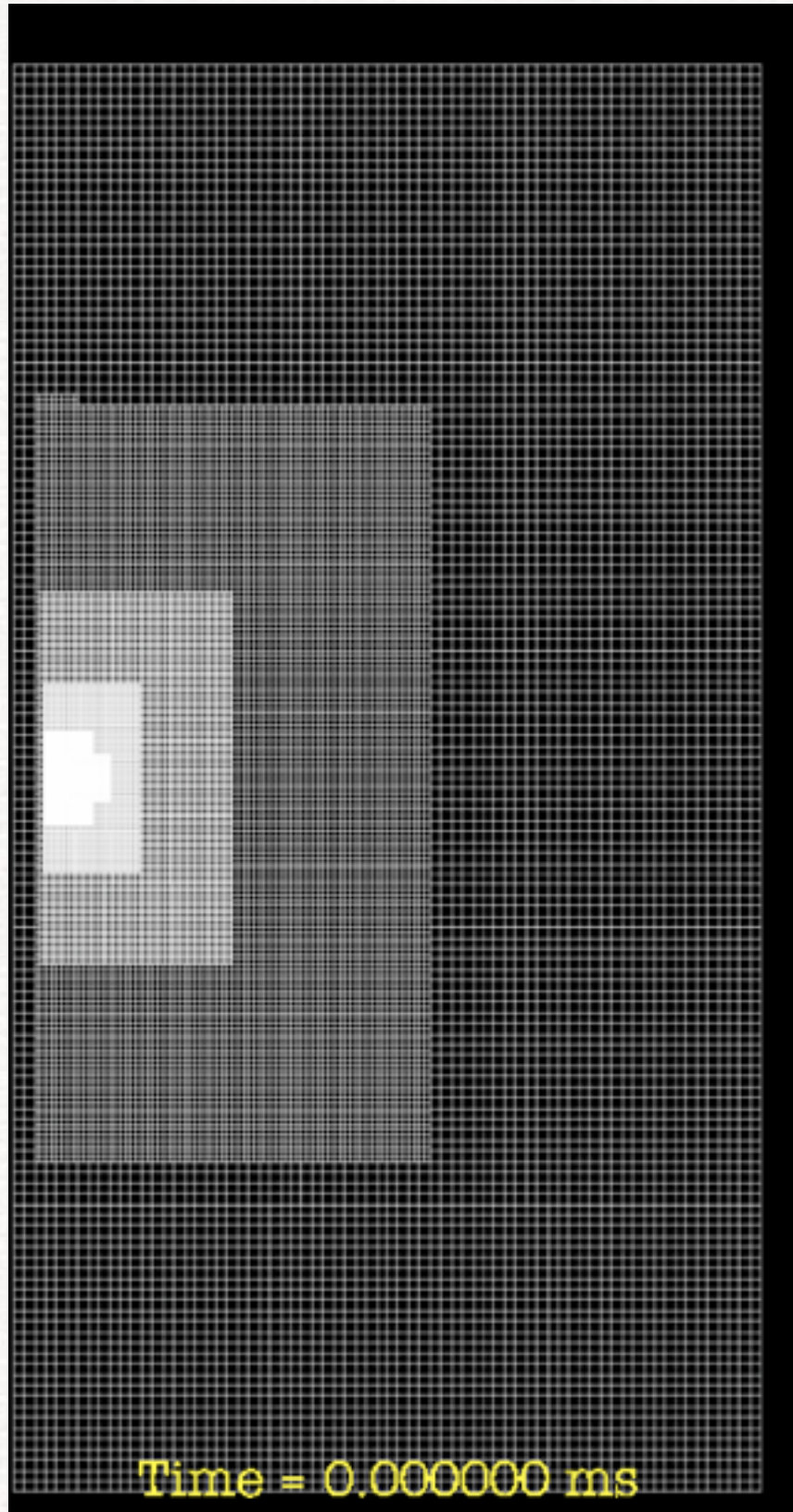
Ideal-fluid EOS. Outer boundary: 240 km. Initial NS separation: 45 km.

PPM for the cell reconstruction. Marquina flux formula.

3rd order Runge-Kutta for time-stepping.

The grid hierarchy for the simulations is handled by the CARPET mesh refinement driver.

AMR and grid hierarchy



Grid Setup:

6 refinement levels. Outer boundary: 240 km

Grid spacing from coarsest to finest (km):
6.0, 3.0, 1.5, 0.75, 0.375, 0.1875

Size individual moving grids (coarsest-to-finest;
km): 240, 180, 120, 60, 30, 15.

Grid points (finest level):

$(2 * 15 / 0.1875)^3 = 4,096,000.$

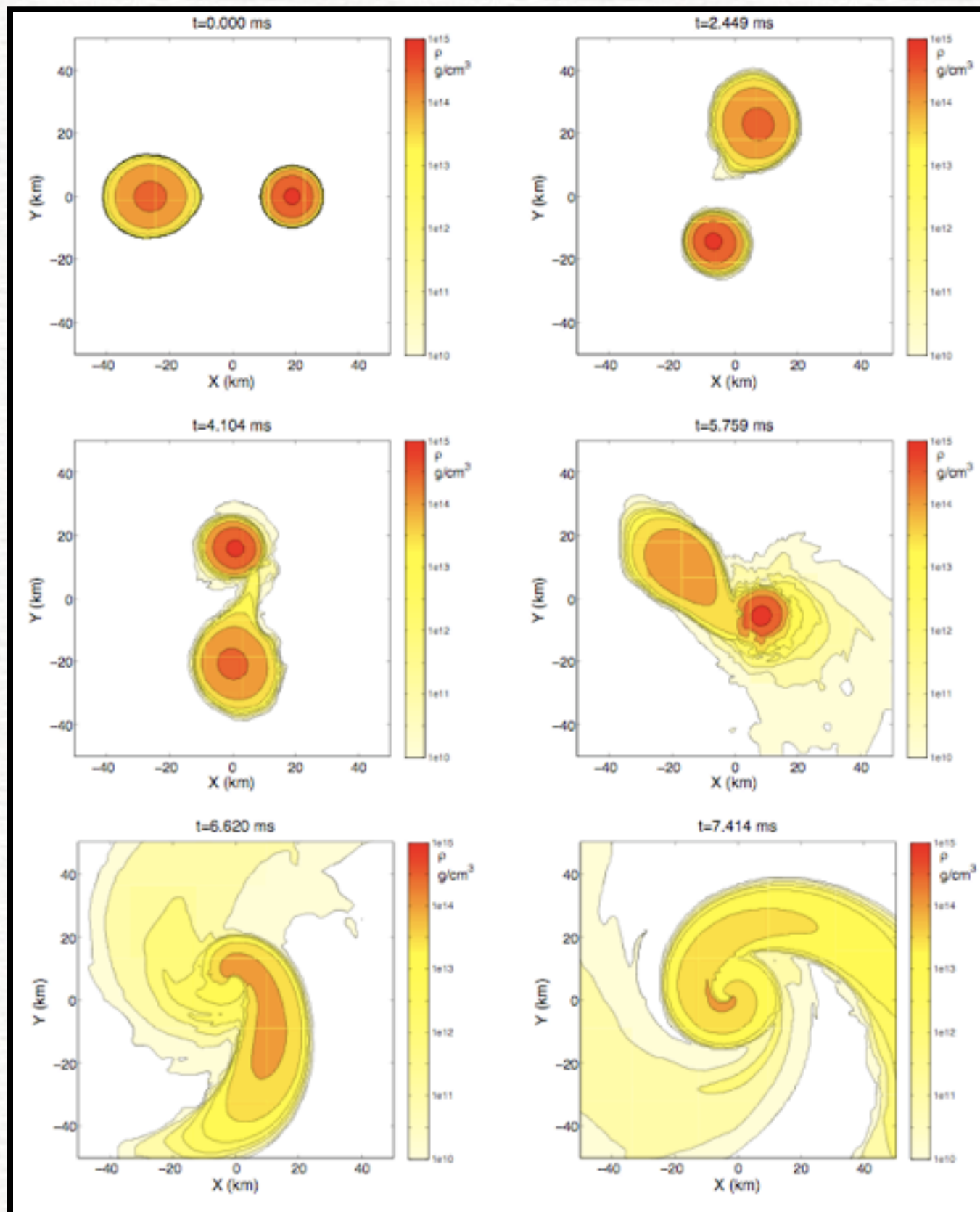
Grid points (coarsest level):

$(2 * 240 / 6)^3 = 512,000.$

Memory requirements: ~170 GB of total memory usage (140 cores on Mare Nostrum)

Duration: 140 cores. Average runtime ~260 hours ~36,400 CPU hours/run. (high-res runs ~ 10^5 CPU hours/run)

General dynamics: model M3.4q0.70



Asymmetry of the system already apparent at initial time.

During the inspiral phase, the heavier and more compact star is only slightly affected by its companion, whereas the latter is decompressed rapidly while being accreted onto the heavier star. (3 intermediate panels)

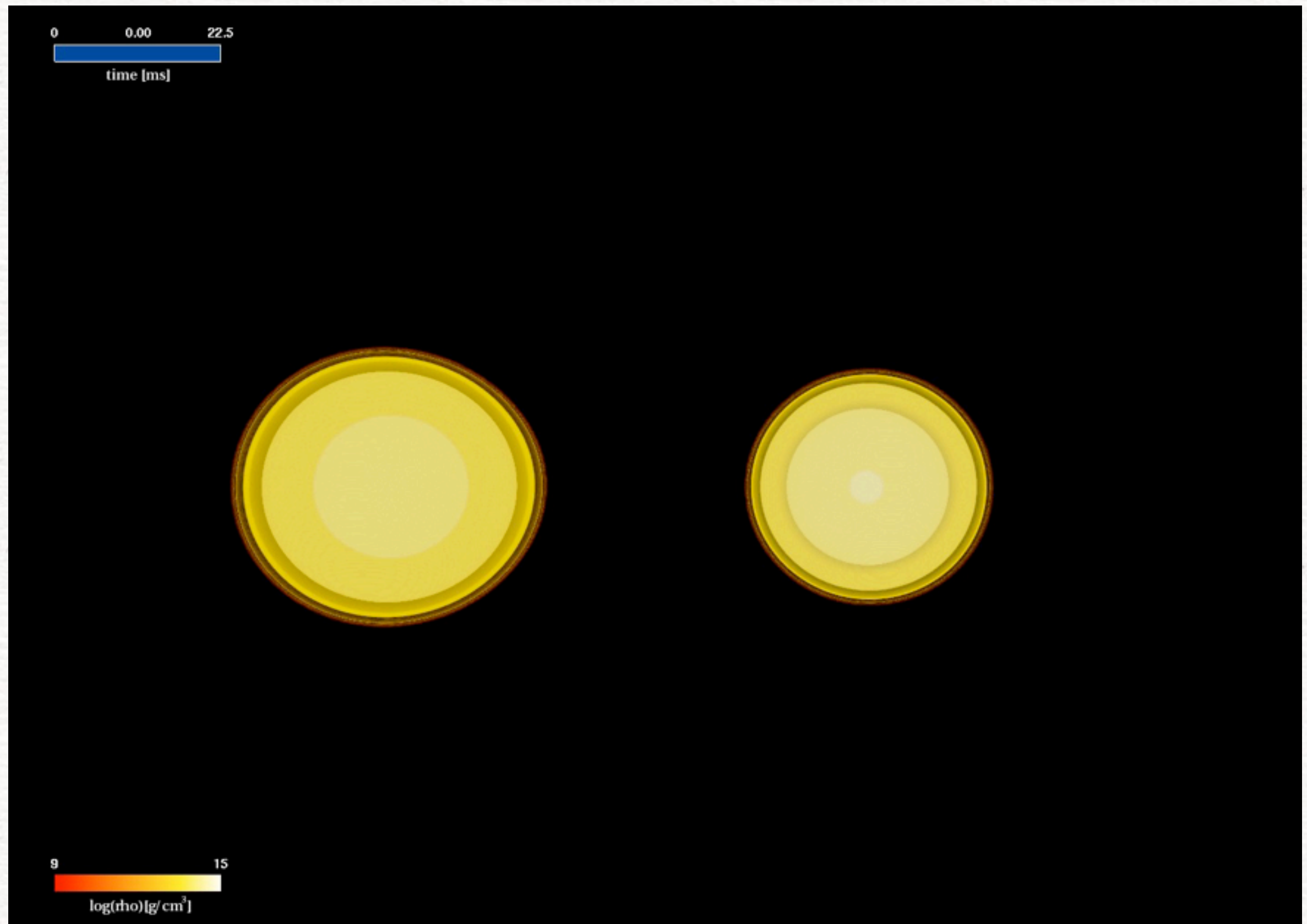
Extended tidal tail, which transfers angular momentum outwards in a very efficient way. **Massive accretion torus formed around the central BH.**

Measured properties of the BH:

kick velocity = 15.82 km/s

Mass of the disk: $0.2 M_{\text{sun}}$

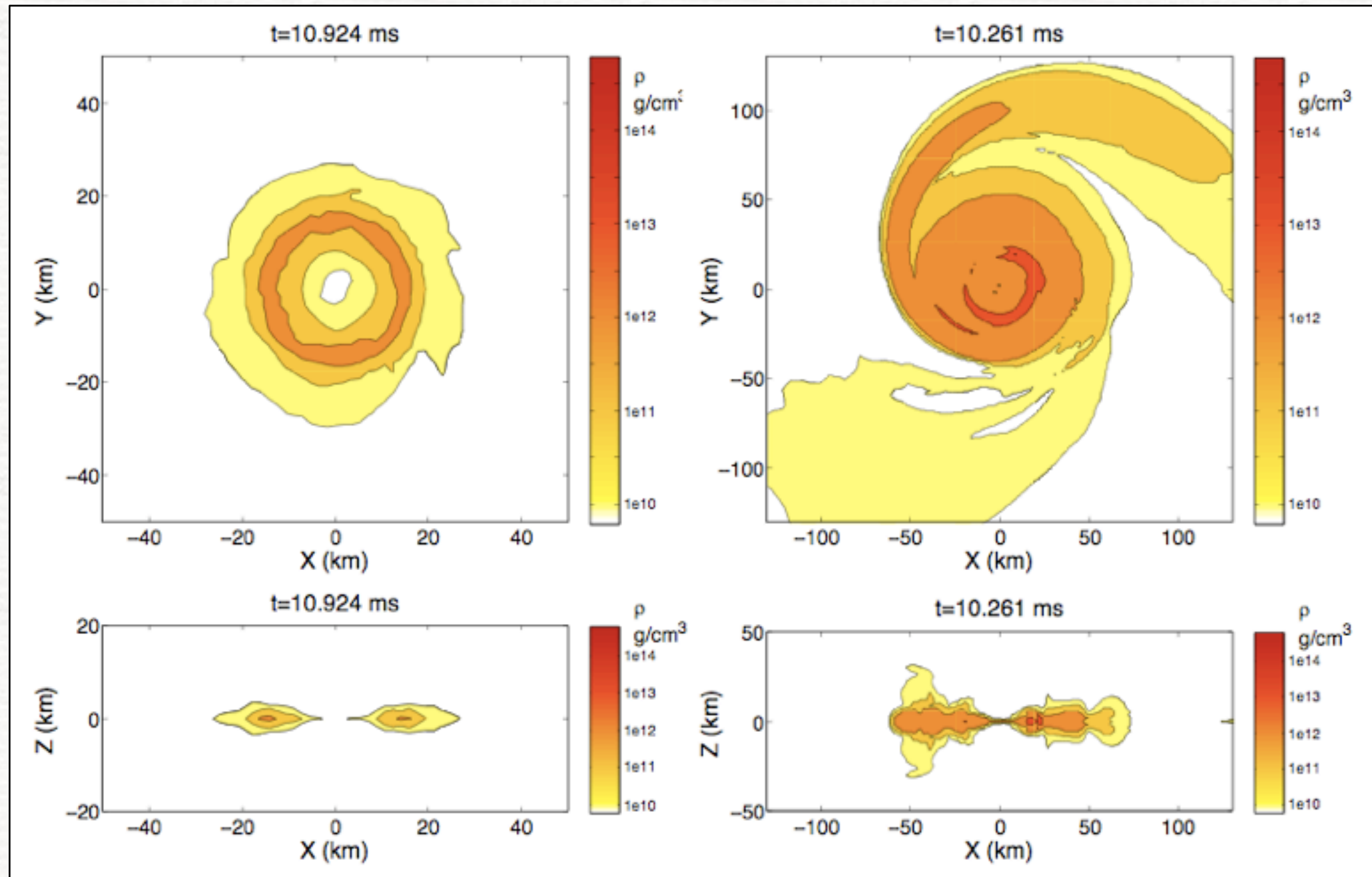
Unequal-mass dynamics: animation



Morphological differences (at onset of QSA)

M3.6q1.00

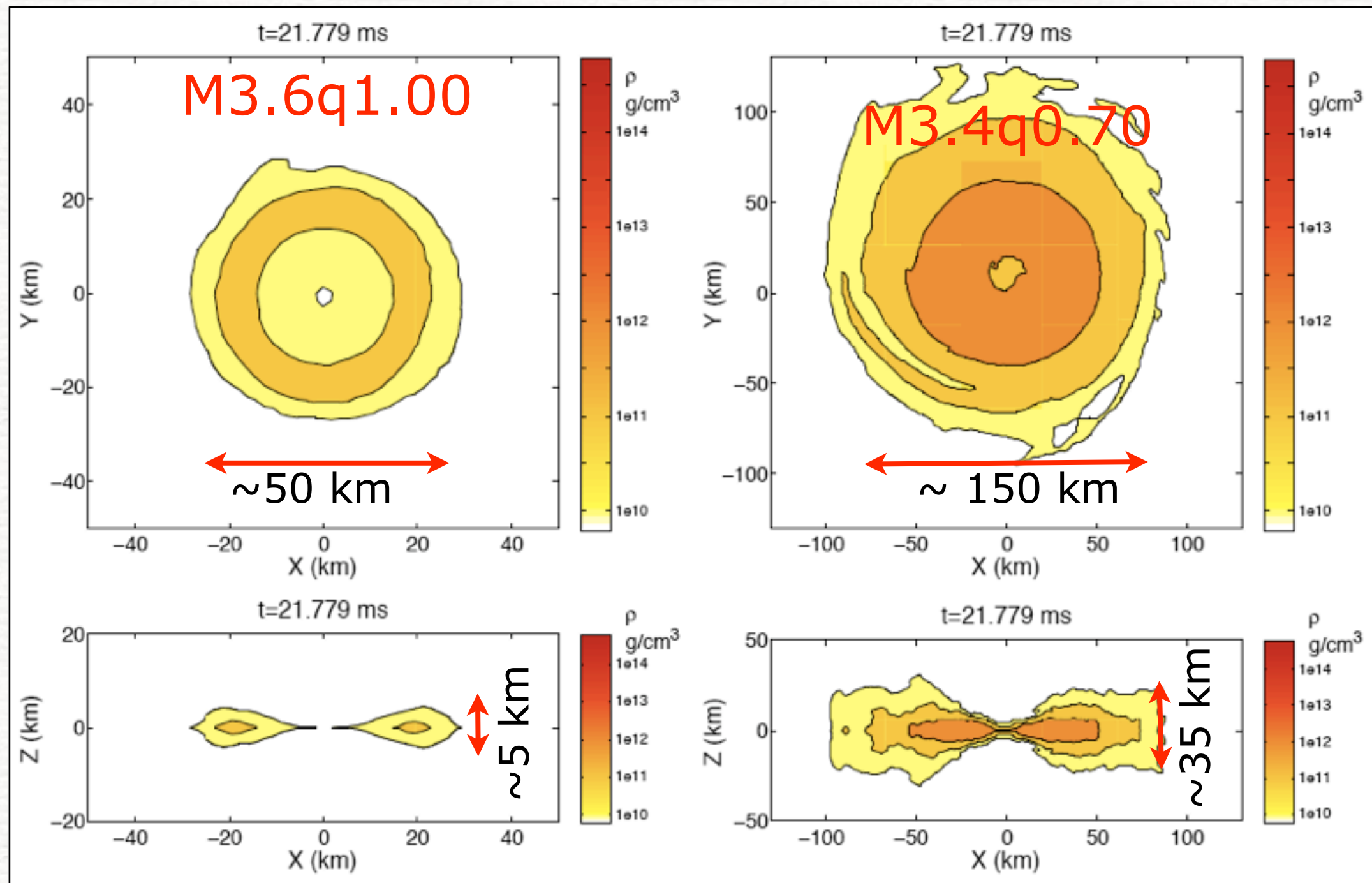
M3.4q0.70



Highly symmetric disk.
Geometrically thin.

Large asymmetry, spiral arm
not yet accumulated onto
central disk surrounding BH.

Morphological differences (at end of simulation)

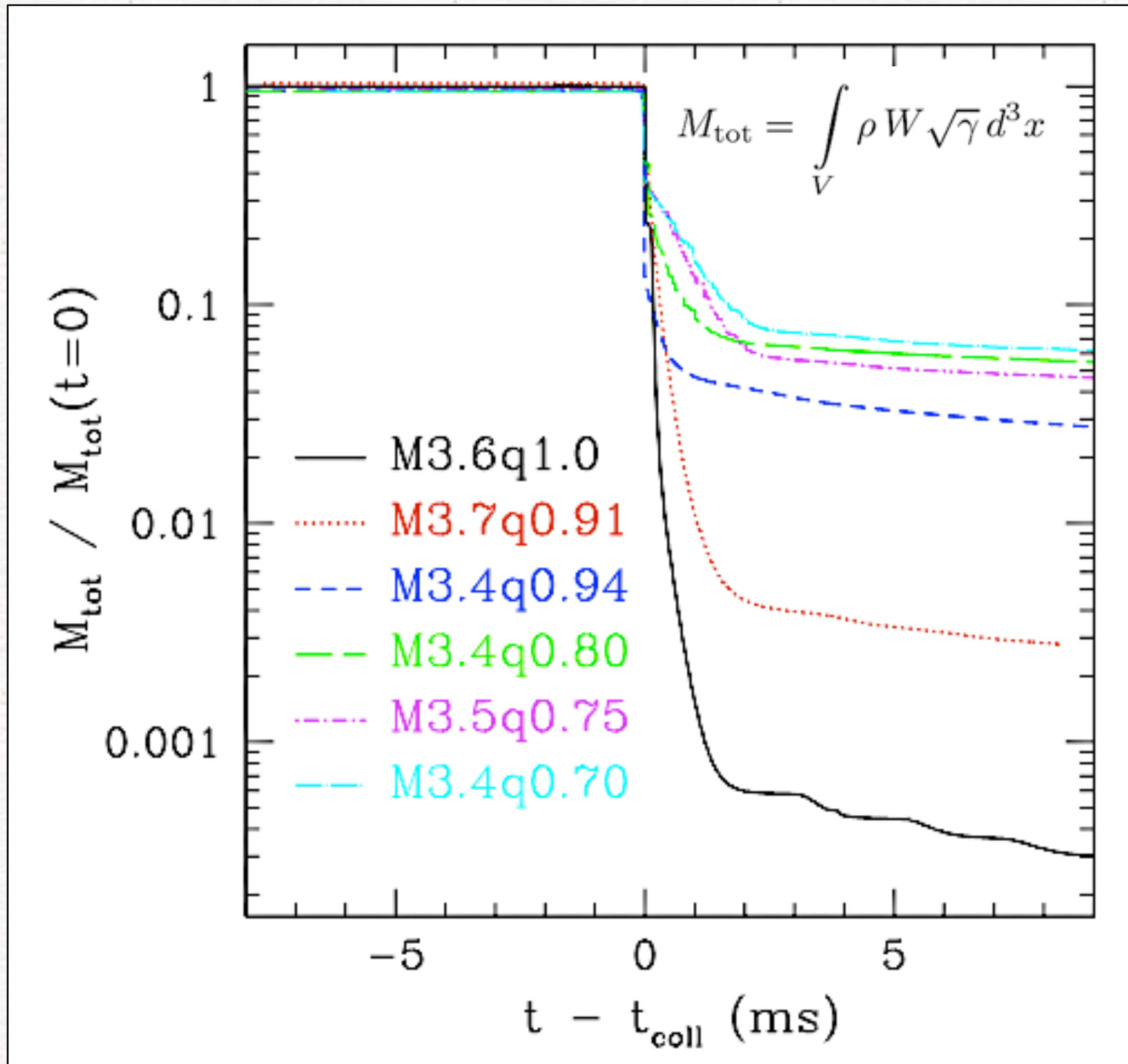


Symmetric. Thin disk.

Axisymmetric shape. Thick disk.

Both tori differ in size by about a factor ~ 3 and in mass by about a factor ~ 200 . However, they have comparable mean rest-mass densities.

Evolution of total rest mass



Curves shifted in time to coincide at collapse time.

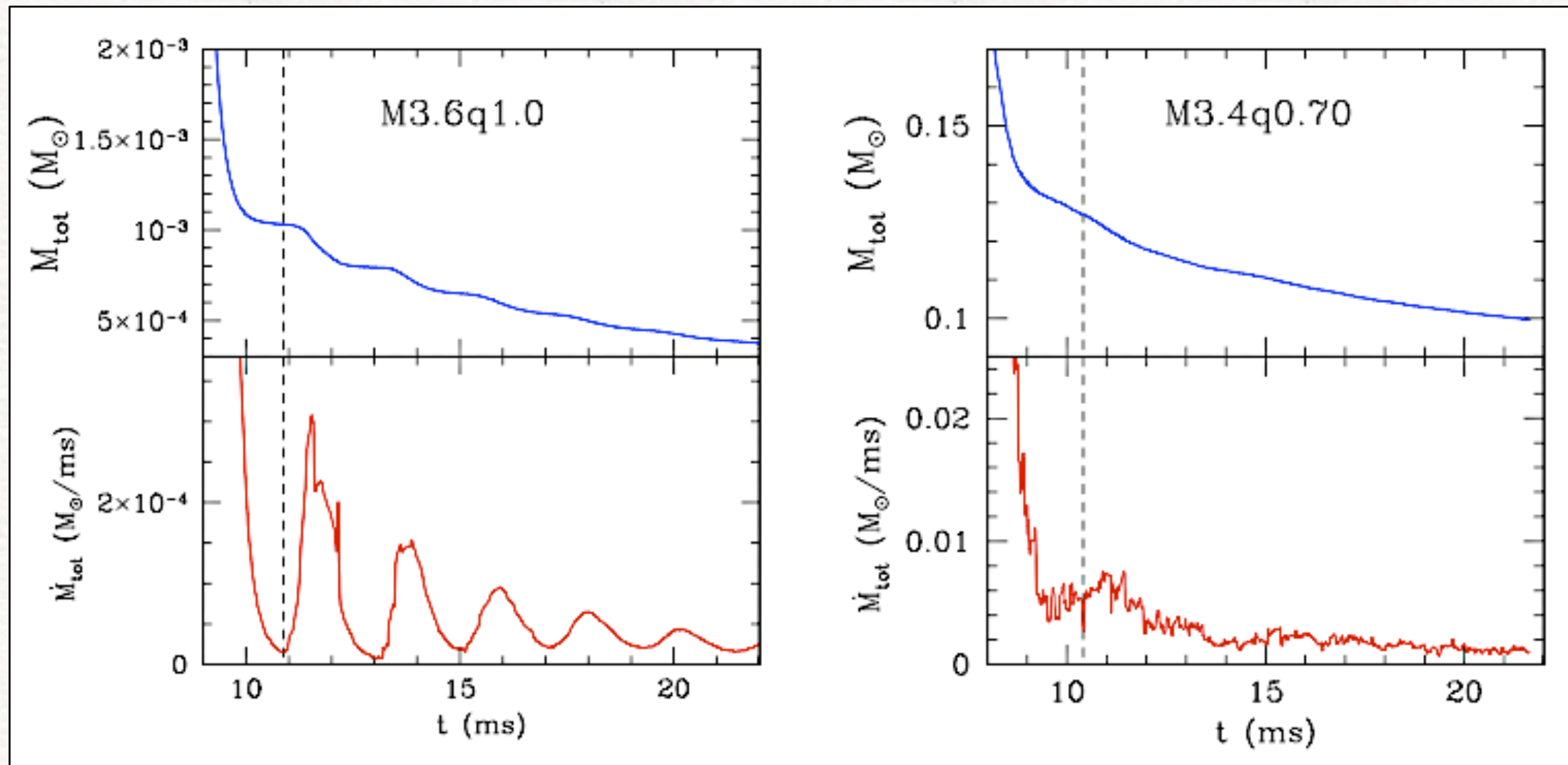
Mass of resulting disk is larger for smaller values of q .

Trend not entirely monotone as it is also influenced by the initial total baryonic mass of binary.

| Model | M_{tor} (M_{\odot}) |
|-----------|-------------------------------------|
| M3.6q1.00 | 0.0010 |
| M3.7q0.94 | 0.0100 |
| M3.4q0.91 | 0.0994 |
| M3.4q0.80 | 0.2088 |
| M3.5q0.75 | 0.0802 |
| M3.4q0.70 | 0.2116 |

Evolution of total mass and accretion rate

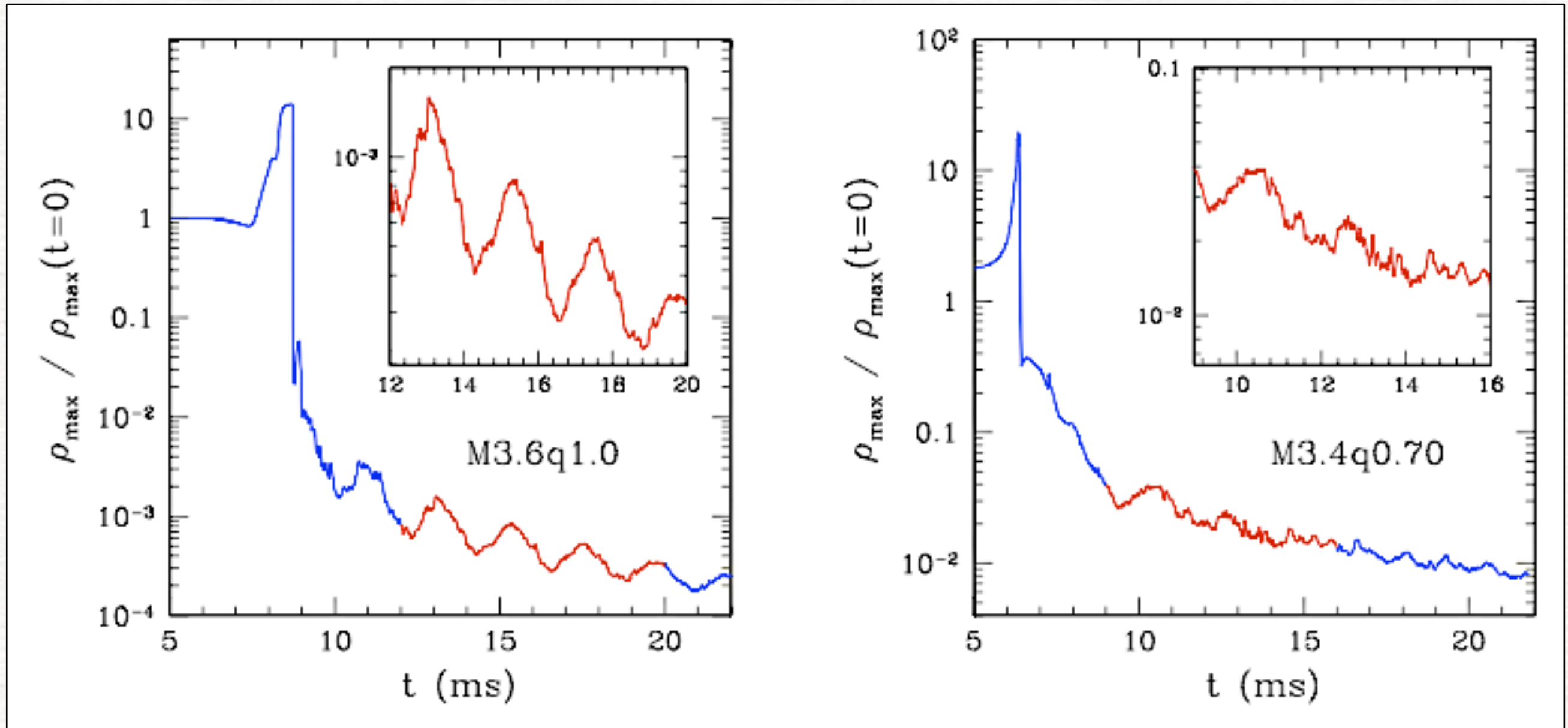
The **torus mass** is defined as the total rest mass outside the AH when the disk enters a regime of quasi-steady accretion (**QSA**). The onset of the QSA is defined as the point in time when the condition mass flux / total mass $< 10^{-6}(\text{Gc}^{-3}\text{M}_{\odot})^{-2}$ is satisfied for the first time.



Equal-mass model shows an accretion rate that is subject to **quasi-periodic oscillations** as the torus moves in and out at about the radial epicyclic frequency.

The mass flux of the **unequal-mass model** is rather **constant in time** and this reflects a very different distribution of angular momentum in the tori.

Evolution of rest-mass density



Harmonic behaviour also apparent in the evolution of the maximum of the rest-mass density.

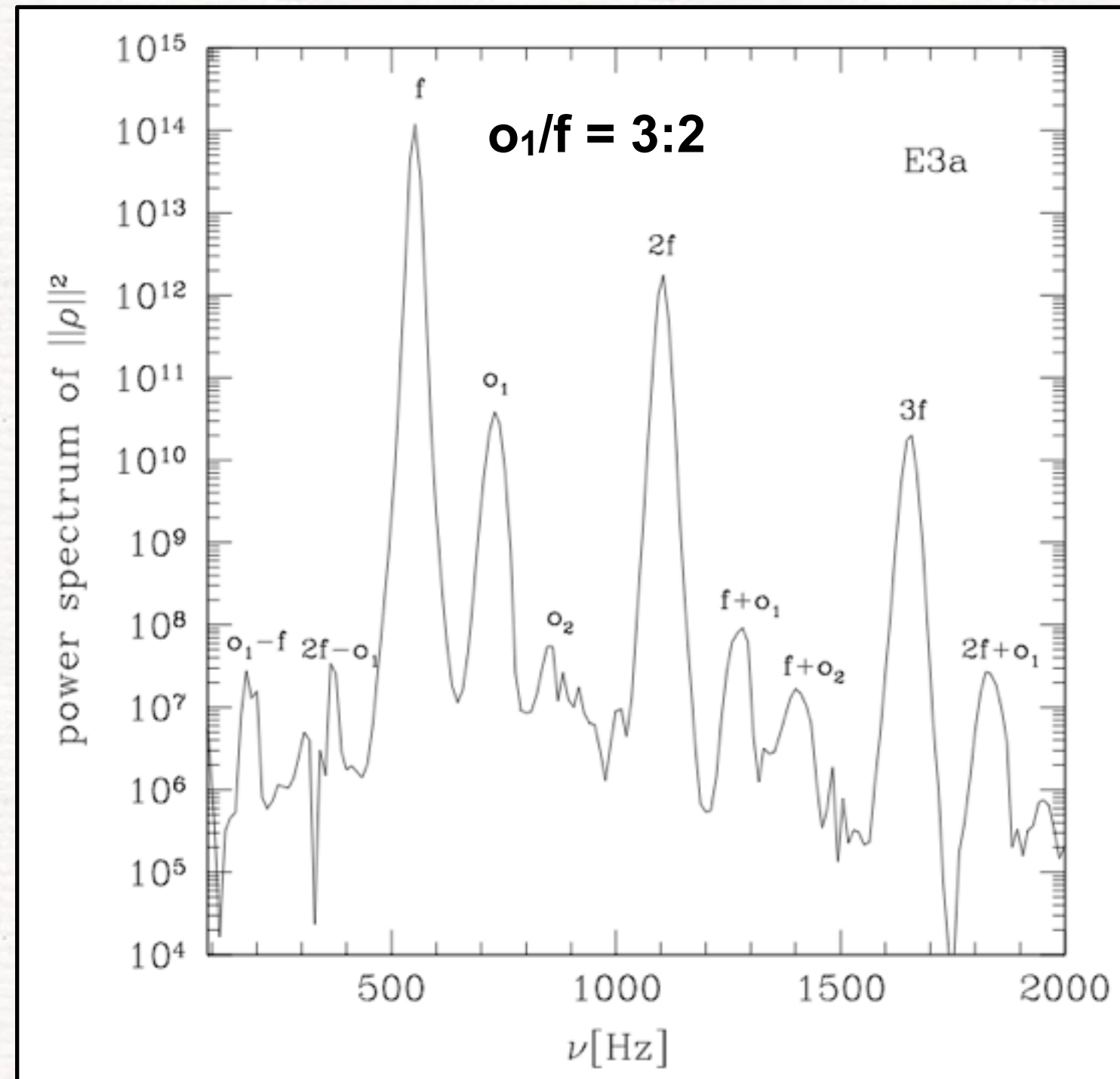
p-mode oscillations of relativistic tori (**test-fluid**)

Our self-consistent simulations lead to disks showing harmonic behaviour in the accretion process.

The dynamics of oscillating relativistic tori in equilibrium analyzed extensively (Rezzolla et al 2003; Zanotti et al 2003, 2005; Montero et al 2007) in the **test-fluid approximation**, with and without magnetic fields, and for the cases of Schwarzschild and Kerr BHs.

Upon the introduction of perturbations in the tori, a **long-term oscillatory behavior** is found, lasting for tens of orbital periods.

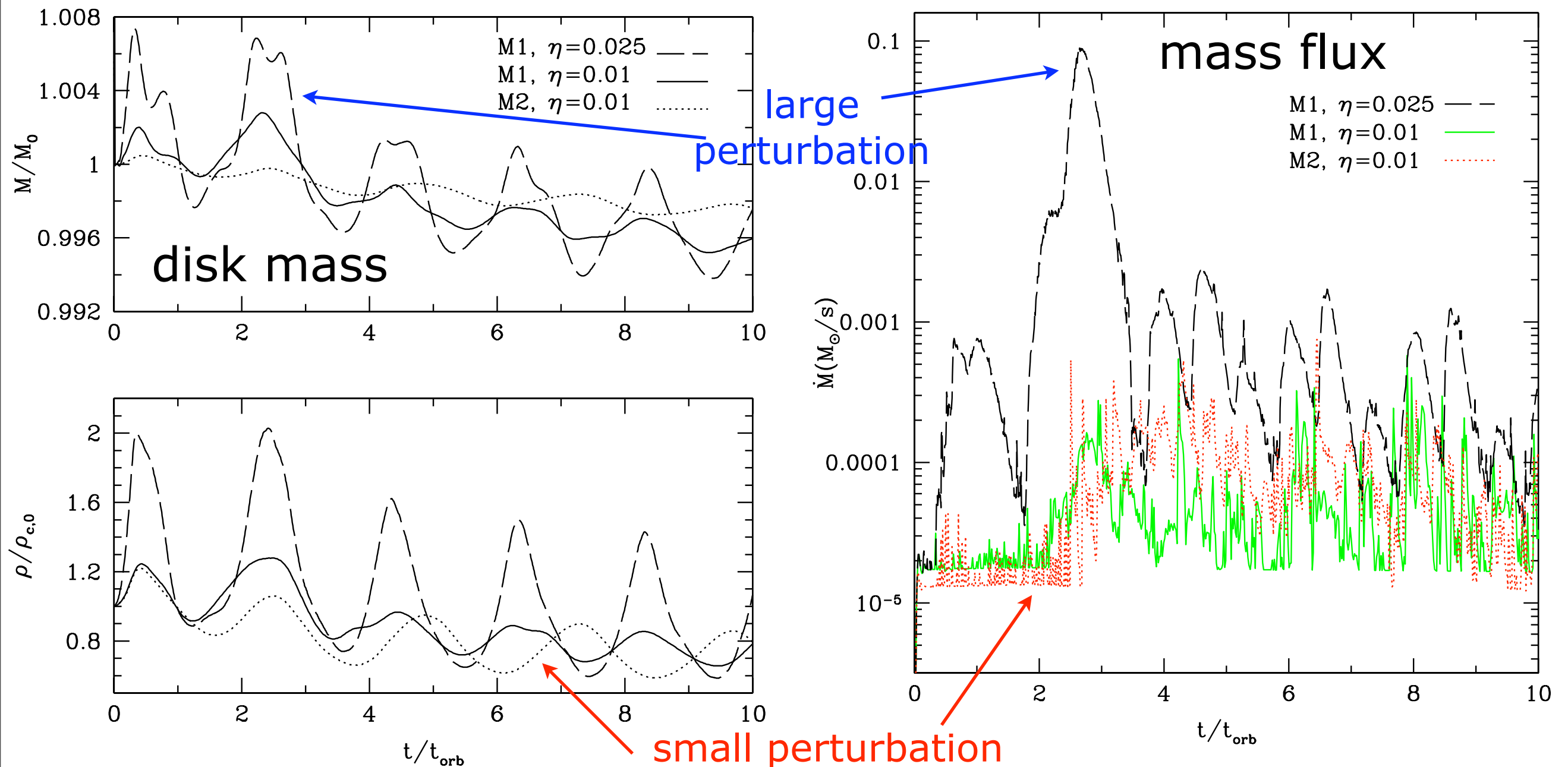
These oscillations correspond to **axisymmetric p-mode oscillations** whose lowest-order frequencies appear in the **harmonic sequence 2:3**.



Zanotti, Font, Rezzolla & Montero (2005)

p-mode oscillations of **self-gravitating** tori

Those studies have been extended by Montero, Font & Shibata (2010), where systems formed by a BH (in the puncture framework) surrounded by (marginally stable) **self-gravitating disks** were evolved in axisymmetry. Even in this case, the ratio of the fundamental oscillatory mode and the first overtone also shows approximately the **2:3 harmonic relation** found in earlier works.

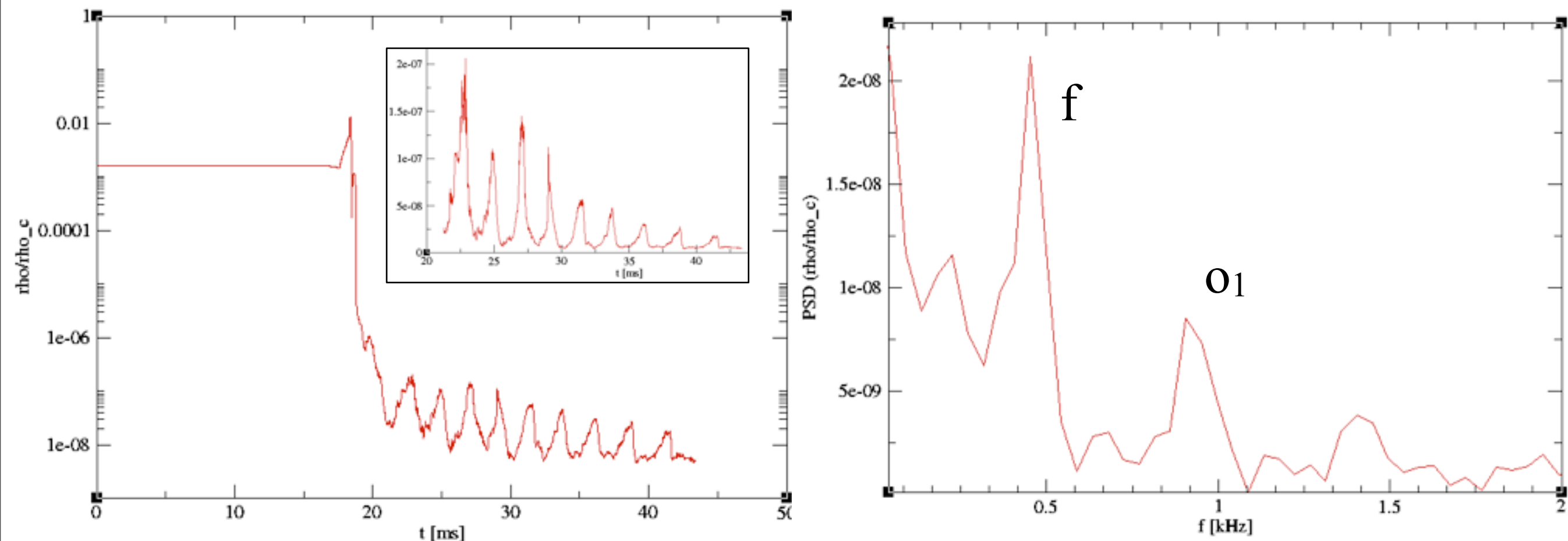


p-mode oscillations of **tori** from **NS mergers**

The dynamics of the BH–torus system produced by the merger of model [M3.6q1.00](#) is more complicated than that considered in the test-fluid studies, for which initial configurations in stable equilibrium exist.

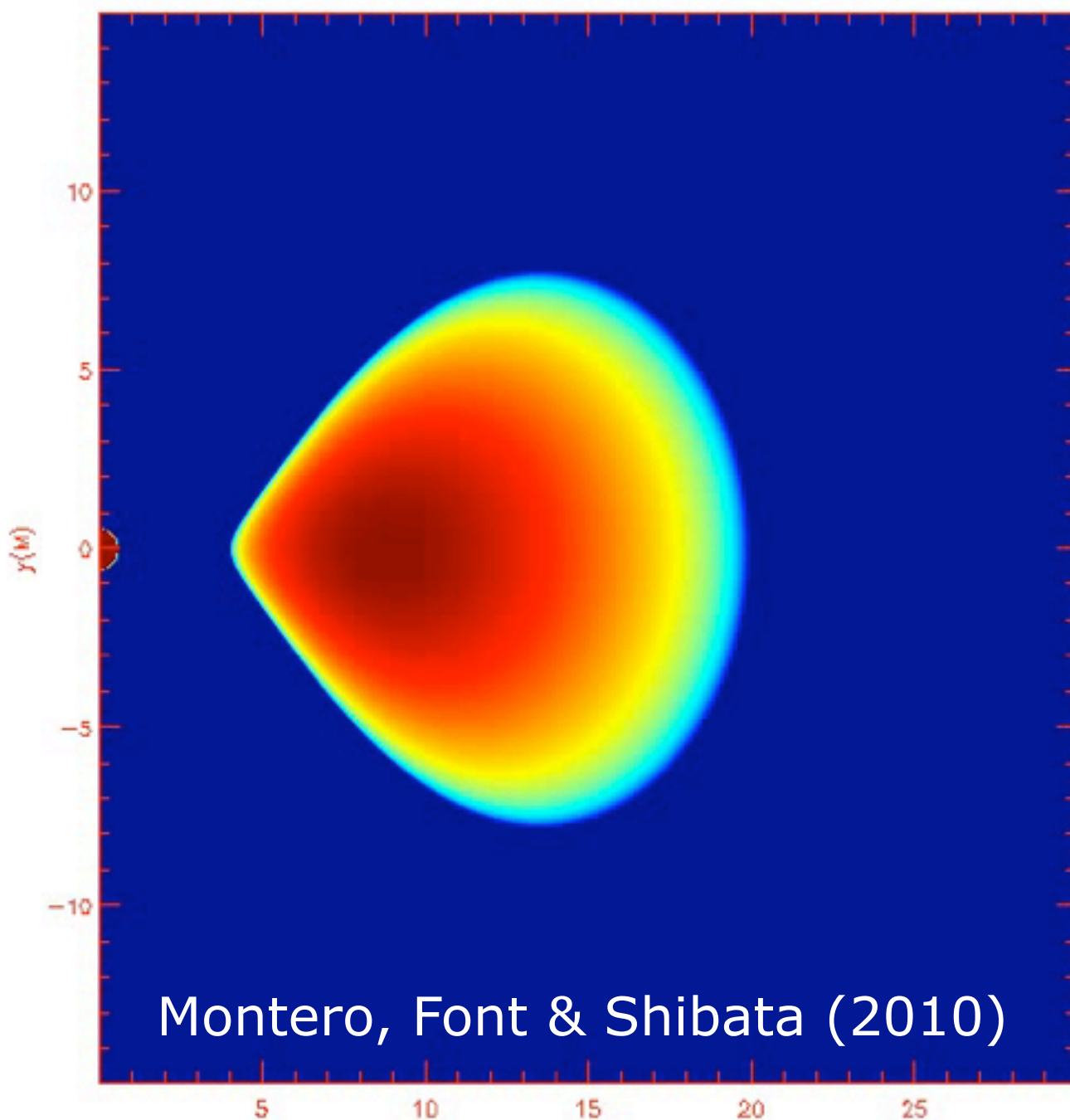
Our systems studied *ab-initio* as the end-products of highly dynamical events, yet so much of the phenomenology found in previous works also applies here.

Timeseries much too short to provide a firm evidence of the presence of the 2:3 harmonic relation. Spectral analysis **excess power present at such frequencies.**



Dynamical instabilities

A **stable enough BH+torus system surviving for a few seconds** is necessary to be considered a plausible **model of short-hard GRBs**. Any instability which might disrupt the system on shorter timescales, e.g. the **runaway instability**, could pose a problem for the accepted GRB models.



Self-gravitating torus in equilibrium around a black hole ($M_t/M_{BH}=1$).

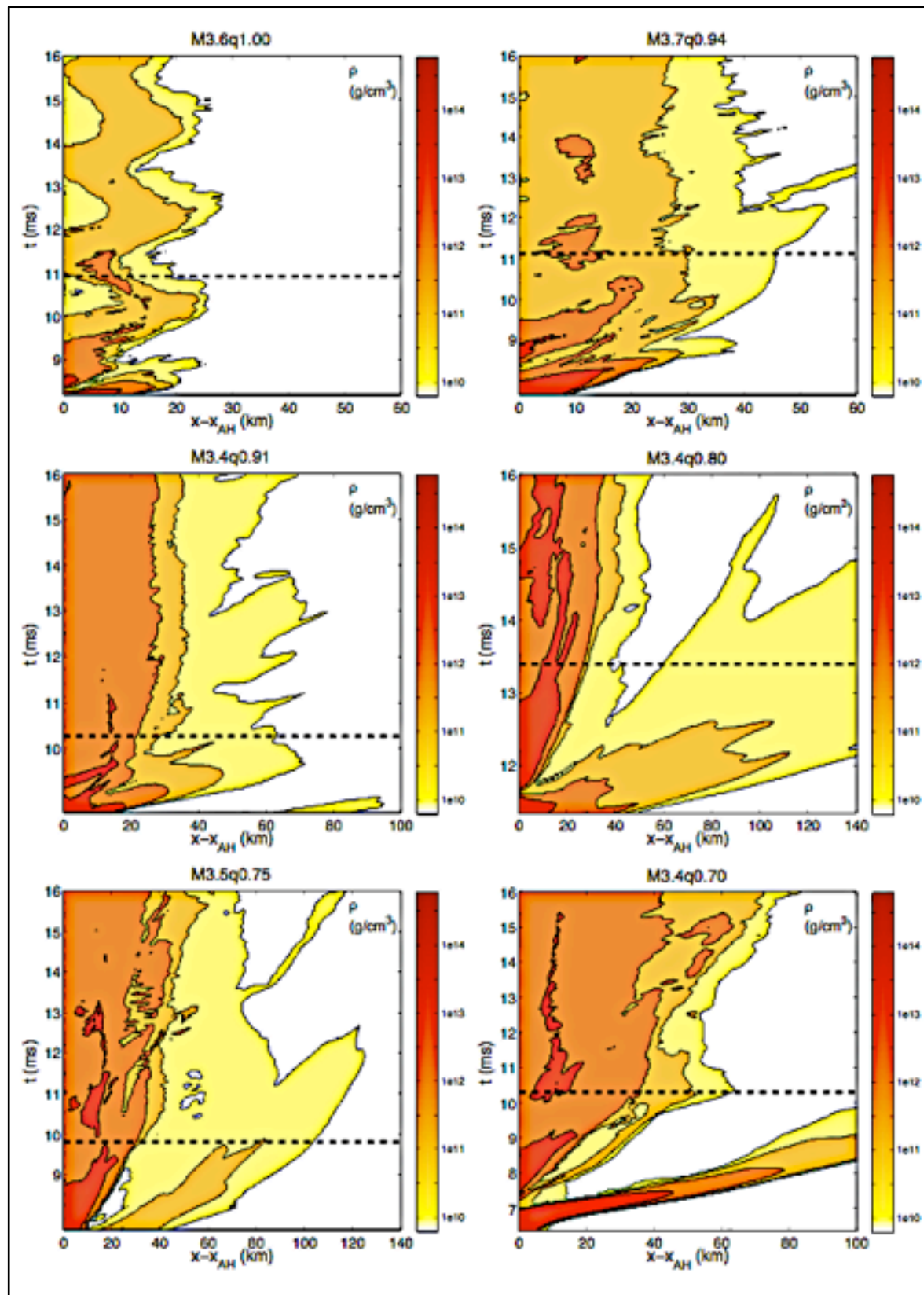
Axisymmetric simulation (2D).

An initial perturbation induces the transfer of small amount of matter through the cusp towards the BH.

This does not reduce significantly the total rest-mass of the torus. At the end of the simulation it is conserved up to about 1%.

Tori are stable irrespective of the angular momentum distribution.

Dynamical instabilities: spacetime diagram



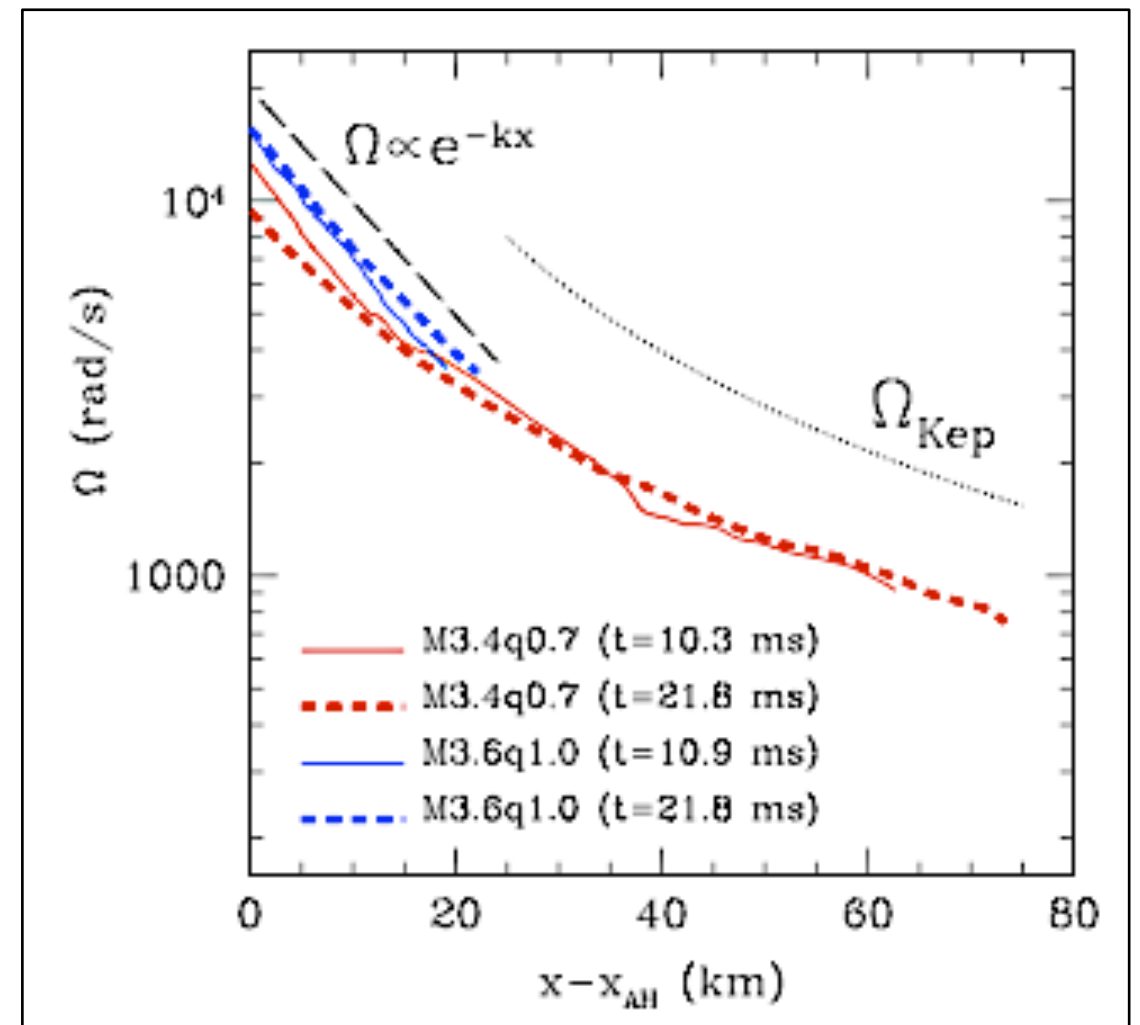
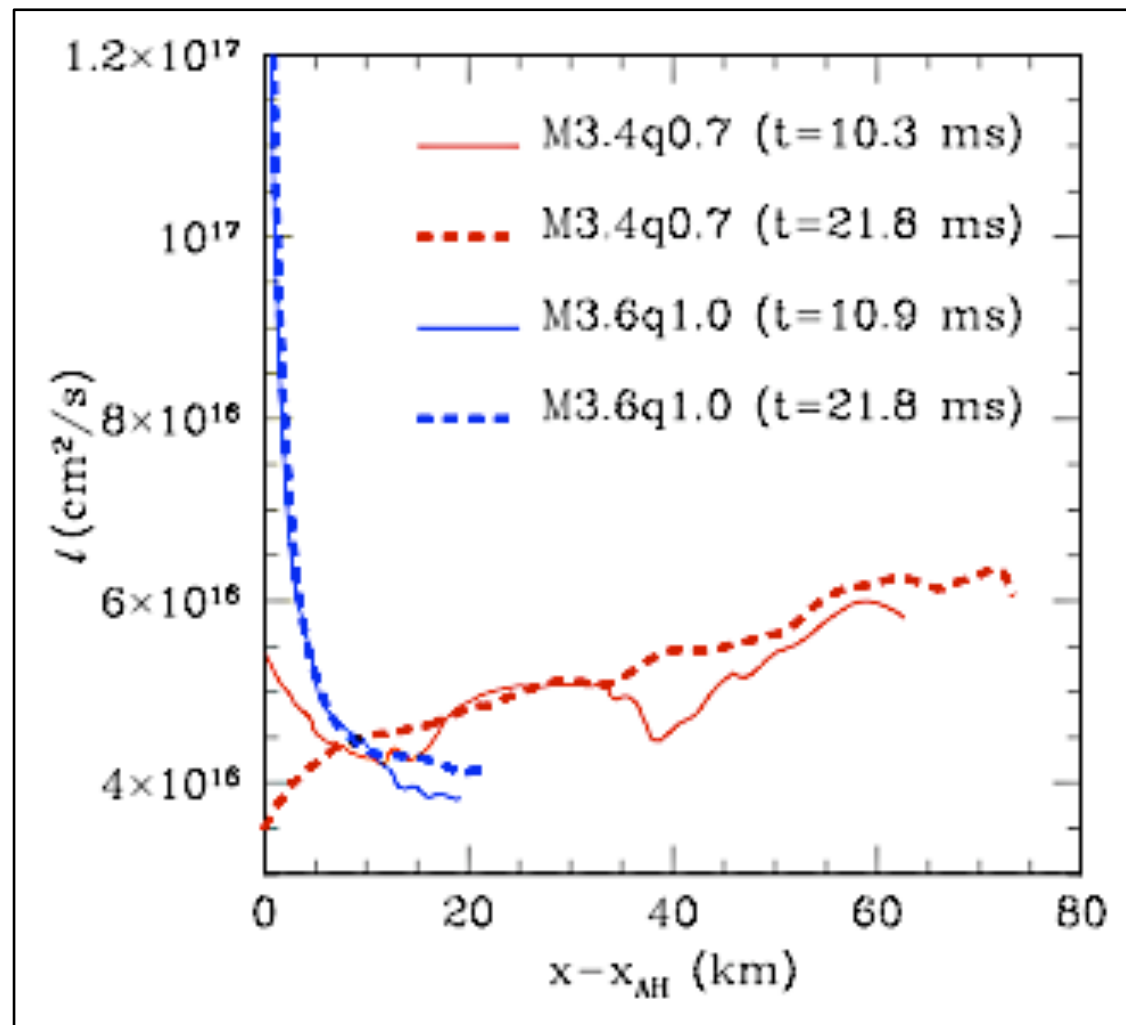
Evolution of the rest-mass density along the positive x -axis in a frame comoving with the BH. Color-coded rest-mass density embedded in a **spacetime diagram**. Dotted horizontal line marks the onset of the regime of QSA.

All our BH+torus systems formed self-consistently as the result of binary NS mergers do not show signs of any dynamical instability, at least on the short dynamical timescales investigated.

Agreement with Montero et al (2010) even though these models are 3D and not restricted to axisymmetry.

On longer timescales $m=1$ instability may set in (Shibata, private communication).

Profiles of angular momentum and angular velocity



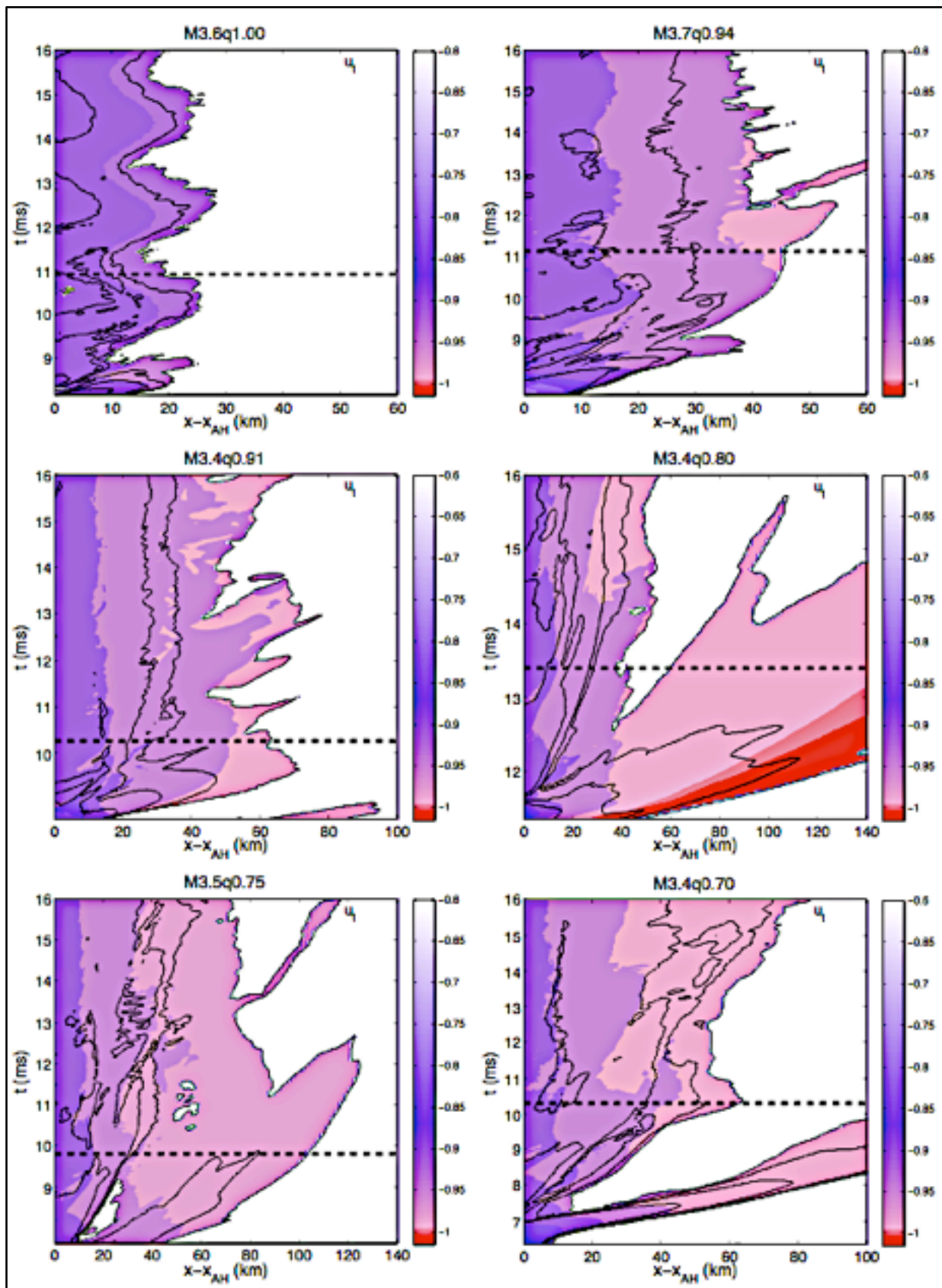
Specific angular momentum decreases outward for the equal-mass binary, while it increases outward for the unequal-mass one.

Rayleigh's dynamical stability criterion (stationary & azimuthal motion) **not satisfied for $q=1$ model.** The stability of this model indicates that this criterion may not be valid for fluids with large radial epicyclic oscillations.

Equal-mass binary has an exponentially decaying profile.

Unequal-mass binary reaches a **Keplerian** profile, $x^{-3/2}$. This explains the scaling of the specific angular momentum as $x^{1/2}$ and provides **firm evidence that the tori produced in this case will be dynamically stable.**

Matter ejection: spacetime diagram of u_t



The local condition $u_t > -1$ provides a necessary, but not sufficient, **condition for a fluid element to be bound**. (The condition is exact only in an axisymmetric and stationary spacetime.)

For almost all models the criterion $u_t > -1$ is well fulfilled. Model M3.4q0.80 shows matter ejection at early times.

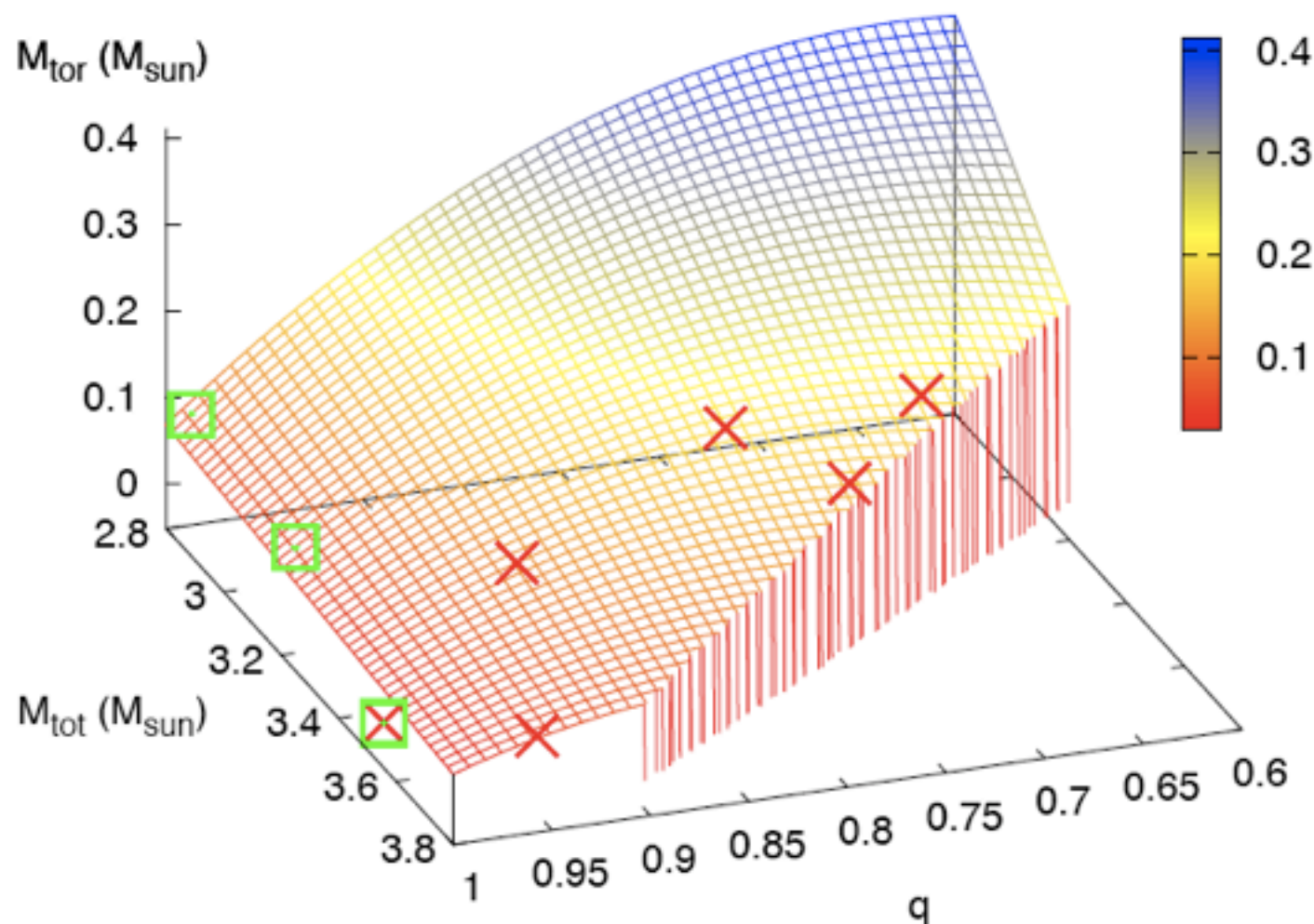
Total amount of matter ejected rather small ($\sim 10^{-4} M_{\odot}$). It can still act as the site for the production of the neutron-rich heavy elements that are formed by rapid neutron capture (i.e. the **r-process**). (Code upgrade with reaction network necessary.)

Mass in the torus

Following Shibata & Taniguchi (2006) we derive a phenomenological expression for the torus mass:

- depends on mass ratio and total mass
- must be smaller than maximum mass of binary system (based on maximum mass of isolated star)
- yield torus with smaller mass for equal-mass binary

$$\begin{aligned}\tilde{M}_{\text{tor}}(q, M_{\text{tot}}) &= c_1(1 - q)(M_{\text{max}} - M_{\text{tot}}) + c_2(M_{\text{max}} - M_{\text{tot}}) \\ &= (c_3(1 + q)M_* - M_{\text{tot}})(c_1(1 - q) + c_2)\end{aligned}$$



Tori with masses as large as $\sim 0.35M_{\text{sun}}$ can be produced for binaries with total masses $\sim 2.8 M_{\text{sun}}$ and $q \sim 0.75 - 0.85$.

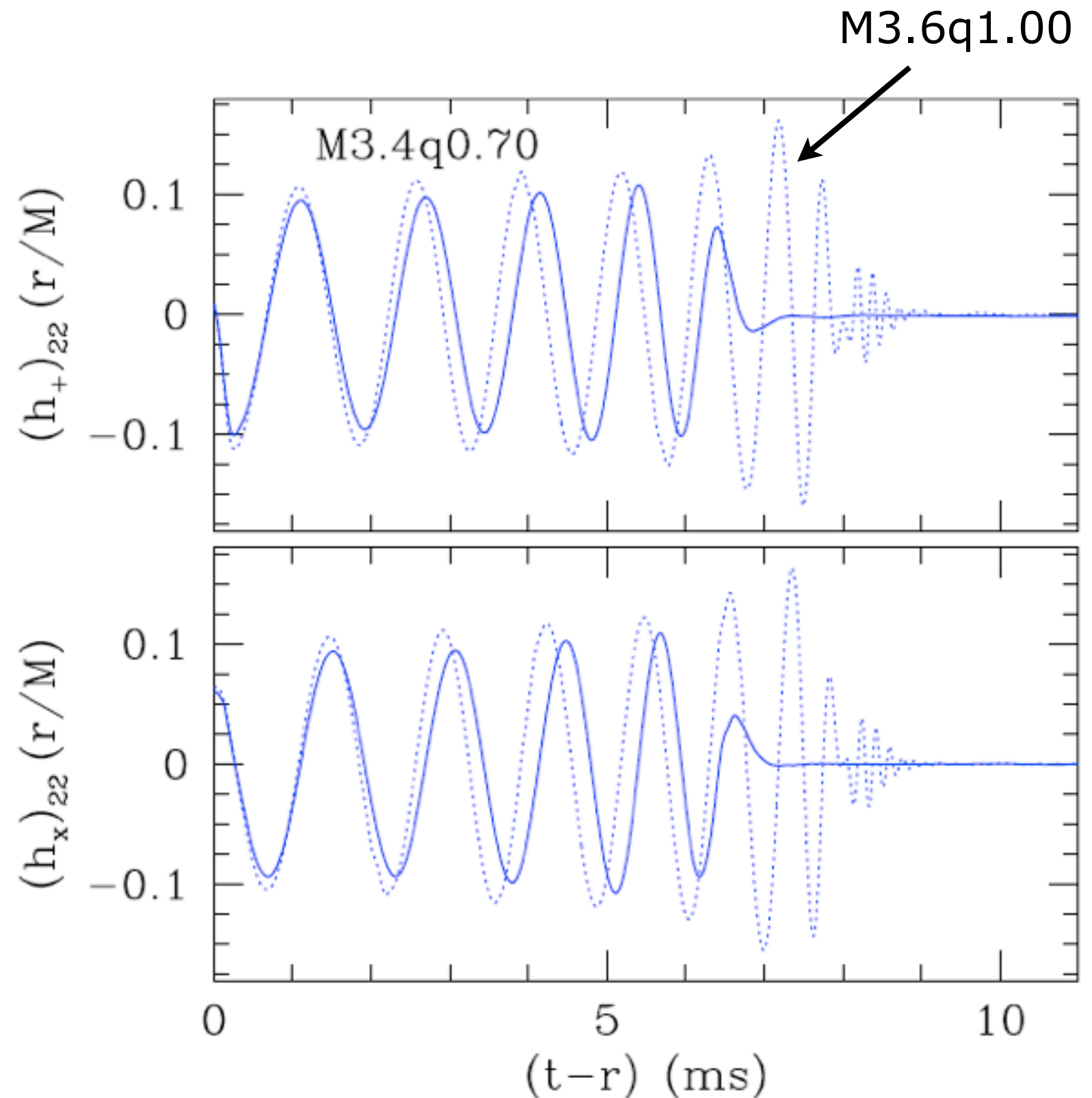
Gravitational wave emission: waveforms

Inspiral phase characterized by **harmonic oscillations** at roughly twice the orbital frequency. Increase both in amplitude and frequency.

Post-merger waveform is basically the one corresponding to the **collapse of the HMNS to a BH**.

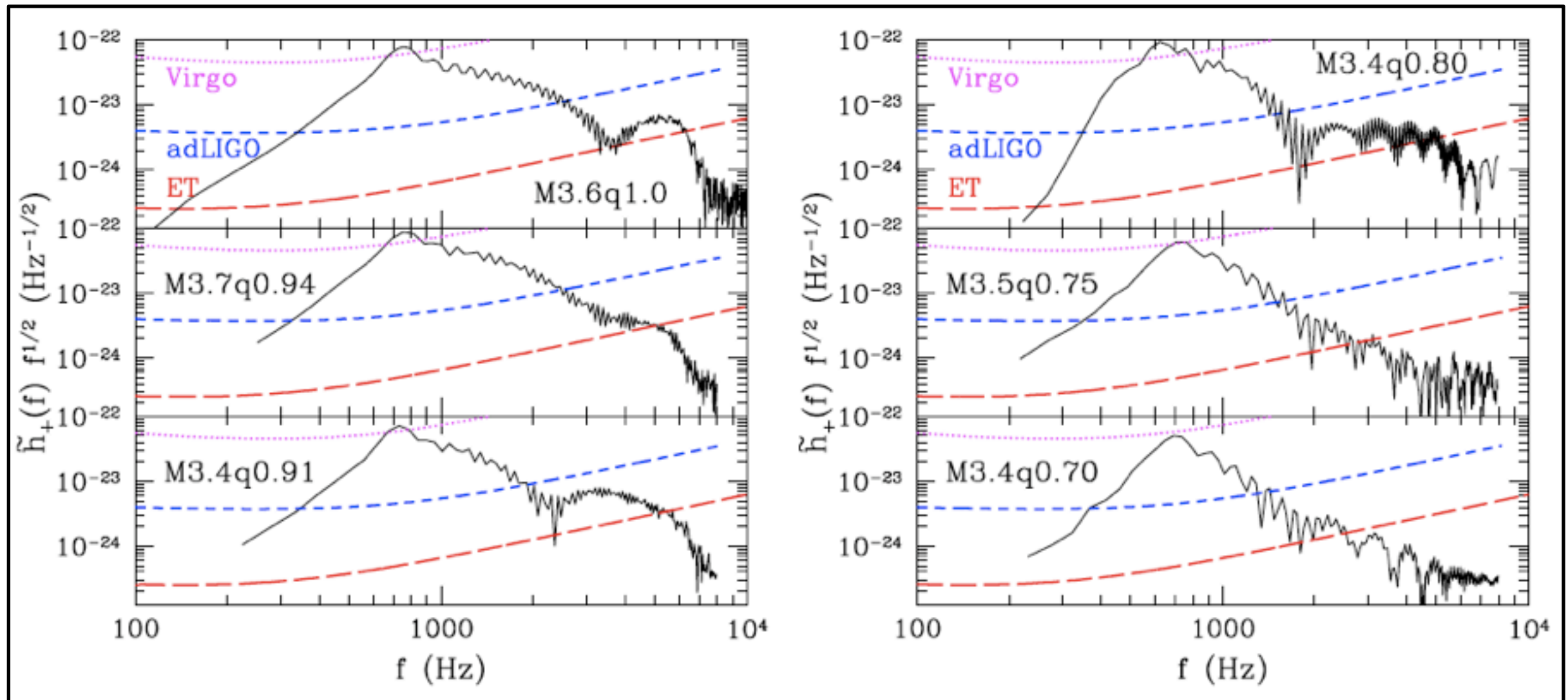
QNM **ringdown signal** starts increasingly early for binaries with smaller mass ratios. Its signature in the waveform **less evident** due to copious mass accretion.

Besides the different amplitude evolution, the mass asymmetry also results into a **different phase evolution** which may provide information on the EOS.



Gravitational wave emission: PSD

Power spectral densities of h_+ for all models when placed @ 100Mpc.



Noise curves of Virgo (magenta), advanced LIGO (blue), and Einstein Telescope (ET) (red). Amplitude depends on the mass ratio: maximal for the high- q binaries and above the noise curve for Virgo in these cases.

New-generation detectors such as advanced LIGO will be able to reveal the inspiral signal in the frequency interval $\sim 0.3 - 2.0$ kHz, while essentially all of the late-inspiral and merger signal would be measured by ET.

Summary of our results

The evolution of unequal-mass binary neutron stars has been followed through the **inspiral phase, the merger and prompt collapse to a BH**, up until the appearance of an **accretion disk**, which has been studied as it enters and remains in a regime of quasi-steady accretion.

- **The mass of the torus increases considerably with the mass asymmetry** and equal-mass binaries do not produce significant tori if they have a total baryonic mass larger than $3.7 M_{\text{sun}}$. Those produced have mass $\sim 10^{-3} M_{\text{sun}}$ and a radial extension of ~ 30 km.
- Tori with masses as large as $\sim 0.2M_{\odot}$ have been measured with binaries having $M_{\text{tot}} \sim 3.4 M_{\odot}$ and mass ratios $q \sim 0.75 - 0.85$. The tori in these cases are much more extended with typical sizes > 120 km.
- The mass of the torus can be described accurately by a simple expression involving the maximum mass for the binaries and some coefficients, both of which can be constrained from the simulations. Using the phenomenological expression we conclude that **tori with masses as large as $\sim 0.35M_{\text{sun}}$ can be produced for binaries with total masses $\sim 2.8 M_{\text{sun}}$ and $q \sim 0.75 - 0.85$.**

Summary of our results

- Tori from **equal-mass binaries exhibit a quasi-periodic form of accretion** associated with the radial epicyclic oscillations of the tori, while those from **unequal-mass binaries exhibit a quasi-steady form of accretion.**
- When analyzing the evolution of the angular-momentum distribution in the tori, we find **no evidence for the onset of non-axisymmetric instabilities**, that **angular momentum is transported outwards more efficiently for smaller values of q** thus yielding Keplerian angular-velocity distributions, and that **very little of the mass of the tori is unbound.**
- Present gravitational-wave detectors are unlikely to detect any of the binaries considered here if at a distance of 100Mpc and observed only during the final part of the inspiral.
- **Advanced detectors will be able to reveal these sources** even at large distances and measure them with significant SNRs in the case of third-generation detectors such as ET.